Charles University

Faculty of Science, Department of Inorganic Chemistry

Study programme: Chemistry

Branch of study: Inorganic Chemistry

Bc. Filip Horký

Copper(I) complexes with phosphinonitrile donors

Měďné komplexy s fosfinonitrilovými donory

Diploma thesis

Supervisor: prof. RNDr. Petr Štěpnička, Ph.D.

Prague, 2017

Motto:

> The highest happiness of man ... is to have probed what is knowable and quietly to revere what is unknowable.
>
> Johann Wolfgang von Goethe

Declaration

I declare that this Thesis is my original work expect as cited in the references. The Thesis has not been submitted, or is being concurrently submitted, for any other degree.

Prohlášení

Prohlašuji, že jsem tuto závěrečnou práci zpracoval samostatně a že jsem uvedl všechny použité informační zdroje a literaturu. Tato práce ani její podstatná část nebyla předložena k získání jiného nebo stejného akademického titulu.

Jsem si vědom toho, že případné využití výsledků, získaných v této práci, mimo Univerzitu Karlovu je možné pouze po písemném souhlasu této univerzity.

V Praze, 15. 5. 2017

Bc. Filip Horký

Acknowledgements

I would like to express my greatest appreciation to my supervisor prof. RNDr. Petr Štěpnička, Ph.D., for his inspiring advices, kind attitude and immense patience during the whole time of my study. I would also like to thank RNDr. Ivana Císařová, CSc., for single-crystal X-ray measurements and doc. RNDr. Jiří Mosinger, Ph.D., for luminescence measurements.

I also wish to thank all colleagues from lab no. 316 for everyday help and inspiration, namely to my unofficial consultant RNDr. Karel Škoch, Ph.D., who always knew how to make every project even bigger, to Mgr. Martin Zábranský, the buddy for midnight syntheses, and to Bc. Petr Vosáhlo for his terrible music and movie taste.

Last but not least, I wish to thank my family, teachers and friends for their support, tolerance and patience during my study.

The research presented in this Thesis was financially supported by the Czech Science Foundation (project no. 13-08890S).

Title: Copper(I) complexes with phosphinonitrile donors

Author: Bc. Filip Horký

Department: Department of Inorganic chemistry

Supervisor: prof. RNDr. Petr Štěpnička, Ph.D.

Abstract: Although coordination compounds with phosphinonitrile ligands are already well known, in the vast majority of these complexes these ligands coordinate as simple P-donors with their cyano groups acting as auxiliary substituents. This led us to synthesize and study a series of Cu(I) complexes with two isomeric phosphinonitrile donors, namely 2-(diphenylphosphino)benzonitrile (L^o) and 2-(diphenylphosphino)benzonitrile (L^p), with different ligand-to-metal ratios and possibly characterize further coordination modes offered by these hybrid donors.

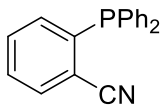

L^o

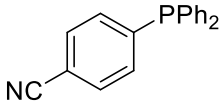

L^p

This work describes the preparation of phosphinonitrile complexes from the aforementioned ligands and simple copper(I) halides (CuX, X = Cl, Br, I), pseudohalides (X = CN) and from $[Cu(MeCN)_4][BF_4]$. The products were characterized by nuclear magnetic resonance, infrared spectroscopy and elemental analysis, mass spectrometry, and their solid-state structures were determined by single-crystal X-ray crystallography.

In addition, luminescent properties of the Cu(I) complexes were studied and catalytic activity of selected complexes was tested in copper-catalyzed alkyne-azide cycloaddition (CuAAC) leading to triazoles.

Keywords: phosphinonitrile ligands; copper(I) complexes; luminescence; catalysis.

Název práce: Měďné komplexy s fosfinonitrilovými donory

Autor: Bc. Filip Horký

Katedra: Katedra anorganické chemie

Vedoucí bakalářské práce: prof. RNDr. Petr Štěpnička, Ph.D.

Abstrakt: Ačkoli byly koordinační sloučeniny obsahující fosfinonitrilové donory již hojně studovány, ve většině připravených komplexů byly tyto ligandy k centrálnímu kovu vázány pouze jako čisté P-donory, tj. s nekoordinovanými nitrilovými skupinami. To nás vedlo k přípravě a studiu komplexních sloučenin obsahující dva isomerní ligandy, 2-(difenylfosfino)benzonitril (L^o) a 4-(difenylfosfino)benzonitril (L^P), při různém poměru ligandu ke kovu s cílem popsat nové koordinační módy.

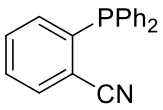

L^o

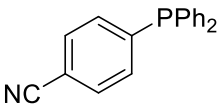

L^p

Předkládaná práce představuje nové měďné komplexy získané reakcemi zmíněných ligandů z jednoduchých halogenidů (CuX, X = Cl, Br, I) a pseudohalogenidů (X = CN) měďných a komplexy iontového typu připravené z prekurzoru $[Cu(MeCN)_4][BF_4]$. Výsledné komplexní sloučeniny byly charakterizovány elementární analýzou, infračervenou spektroskopií, hmotnostní spektrometrií, nukleární magnetickou rezonancí a jejich struktury byly určeny rentgenostrukturní analýzou.

Kromě uvedeného byly studovány i luminiscenční vlastnosti získaných sloučenin a pro vybrané komplexy byla testována jejich katalytická aktivita v mědí katalyzované cykloadici azidu s alkyny (CuAAC), která poskytuje triazoly.

Klíčová slova: fosfinonitrilové ligandy; měďné komplexy; luminiscence; katalýza.

Table of contents

1. Introduction

In 1990, D. Seebach predicted that "the discovery of truly new reactions is likely to be limited to the realm of transition-metal organic chemistry, which will almost certainly provide us with additional »miracle reagents« in the years to come".[1,2] Indeed, no other area of classic synthetic chemistry today offers such innovative possibilities as metal-catalyzed organic transformations. Transition metal-mediated reactions are becoming increasingly more significant not only in the synthesis of complex molecules, but also for structurally simpler, industrially important intermediates.[3]

In spite of the numerous reports concerning new coordination compounds with nowadays popular or even uncommon transition metals and their catalytic properties, copper, one of the oldest transition metals to be used in synthetic organic chemistry, is again attracting the attention of researches worldwide – not only as a cheaper alternative to the generally preferred palladium, but also as an exclusive catalyst for new type of reactions.[4]

In 2001 Sharpless[5] introduced the concept of “click chemistry” as a type of reaction which is modular, wide in scope, gives very high product yields, generates only inoffensive byproducts that can be removed by nonchromatographic methods, and stereospecific (but not necessarily enantioselective). The required process characteristics include simple reaction conditions (ideally, the reaction should be insensitive to oxygen and water), readily available starting materials and reagents, the use of no solvent or a solvent that is benign (such as water) or easily removed, and simple product isolation. Purification (if required) must be possible by nonchromatographic methods (e. g., by crystallization or distillation), and the product must be stable under physiological conditions. Since then, click chemistry has become one of the most common and reliable methods to link molecules covalently, and is finding applications in a variety of disciplines including the chemistry of nanomaterials, chemical biology, drug delivery, and medicinal chemistry.[6]

A typical example of click-type reaction is copper-catalyzed alkyne-azide cycloaddition (CuAAC). The 1,3-dipolar cycloaddition of azides with alkynes was firstly reported by Hüisgen in 1963.[7] However, it did not attract much interest until it was demonstrated that this slow, high temperature and unselective process leading to an equimolar

mixture 1,4- and 1,5-disubstitued 1,2,3-triazole regioisomers, could also be carried out under mild condition using Cu(I) compounds as the catalysts.[6,8] In addition, a dramatic improvement of the regioselectivity is observed, with the 1,4-disubstituted isomer being the only product formed (Scheme 1.1).[9]

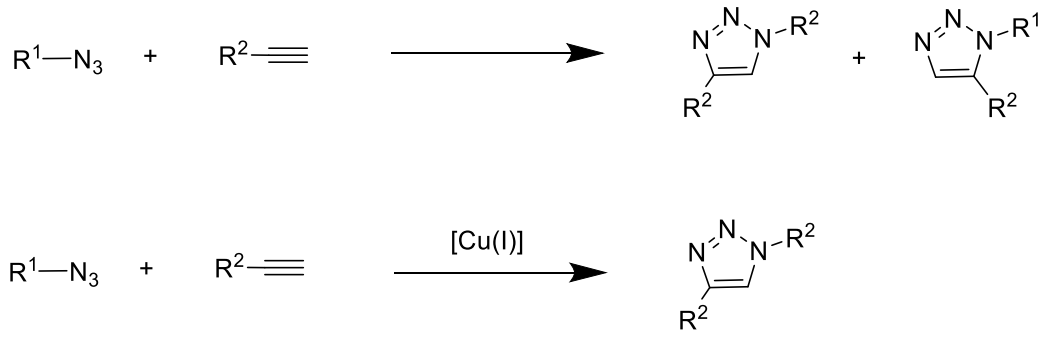

Scheme 1.1: Uncatalyzed (top) and Cu-catalyzed (bottom) synthesis of 1,2,3-triazoles.

Although the final heterocycle does not occur naturally, synthetic molecules containing the 1,2,3-triazole core show interesting chemical and biological properties.[10] 1,2,3-Triazoles are stable to acid and base hydrolysis as well as under reductive and oxidative conditions, which turn suggests their high aromatic stabilization. At the same time, these heterocycles have a high dipole moment (about 5 D)[11] and might be also able to participate actively in hydrogen binds as well as in dipolar and π···π stacking interactions. Finally, this moiety is relatively resistant to metabolic degradation.[12,13] As a result, the CuAAC leading to 1,2,3-triazoles derivates has found valuable applications in drug discovery, dendrimer[14] and polymer chemistry,[15] and also in material science.[16]

There are two main approaches that can be used to prepare a homogenous catalytic system for CuAAC depending on the nature of the catalyst precursor. The most widely used method is *in situ* generation of a Cu(I) species by reduction of $CuSO_4 \cdot 5H_2O$ with sodium ascorbate, typically in a water/alcohol mixture. The major advantage of thus obtained catalysts is compatibility with both oxygen and water. On the other hand, this method is not suitable for substrates sensitive to oxidation and may result in lowered yields associated with Cu(I)-mediated formation of reactive oxygen species.[17,13] For the stabilization of generated Cu(I) oxidative state and acceleration of this reaction were used various auxiliary ligands (for examples, see Scheme 1.2).[18,19,20]

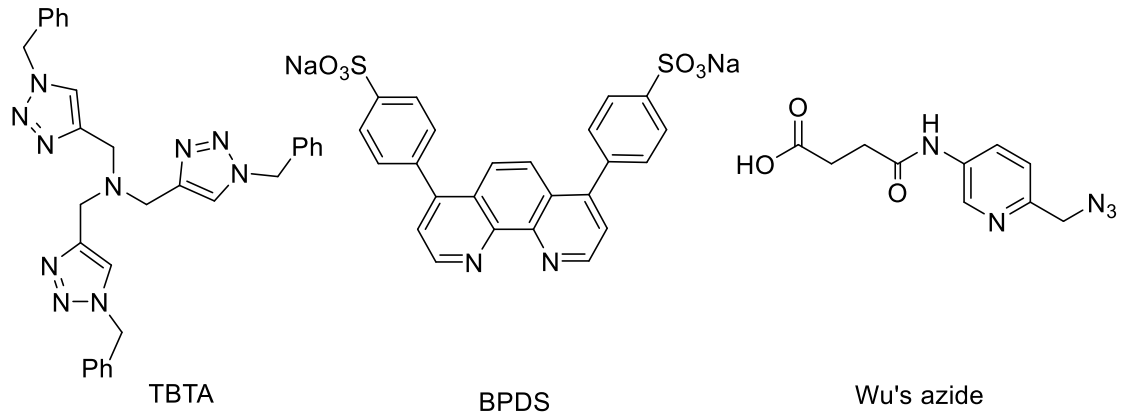

Scheme 1.2: Ligands used in CuAAC reactions: tris(benzyltriazolylmethyl)amine (TBTA),[18] disodium 4,7-diphenyl-1,10-phenanthroline-4',4"-disulfonate (BPDS),[19] and 4-{[6-(azido-methyl)-3-pyridinyl]amino-4-oxo}butanoic acid (Wu's azide).[20]

A different approach makes use of pre-formed Cu(I) complexes as the pre-catalyst. The use of defined catalytic precursors not only avoids the need for an excess of ligand/additives to be present, simplifying the product purification, but also allows a better control over the stereoelectronic properties of the Cu(I) species in the reaction media. Despite this, the simplicity and effectiveness of the Cu(II)/ascorbate prototocol on the one hand, and problems associated with the preparation and handling of air-sensitive Cu(I) compounds on the other hand, have limited applications of defined Cu(I) compounds in CuAAC.[17] However, the number of reports regarding the applications of various Cu(I) pre-catalysts in CuAAC reaction appear to be increasing (Scheme 1.3).[21,22,23]

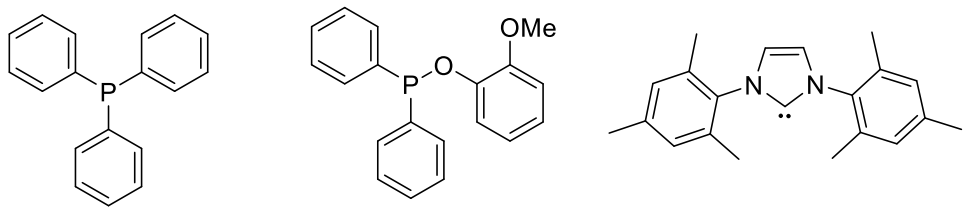

Schema 1.3: Example of compounds used as ligands in defined Cu(I) complexes utilized in CuAAC: triphenyphosphine,[21] 2-methoxyphenyl diphenylphosphinite[22] and *N*,*N*'-bis(2,4,6-trimethylphenyl)-4,5-dihydro-imidazol-2-ylidene (IMes)[23].

The design of a versatile catalyst that can be utilized in cycloaddition of azides to alkynes, no matter their substituents, as well as the improvement of reaction conditions in such a way that copper removal becomes completely effective (eliminating product poisoning) constitutes nowadays some of the challenges that will be probably overcome in the forthcoming years.

However, applications of copper compounds are not limited to CuAAC. Although cross-coupling has almost become synonymous with palladium, copper-mediated reactions were the first of this kind to be reported.[24] For instance, Ullmann reaction, described already in 1901, is a coupling reaction between two aryl halides producing biaryls.[24] Nowadays, the Ullmann-type reactions include nucleophilic aromatic substitutions with various nucleophiles on aryl halides (Scheme 1.4). These reactions, until recently limited in applications by low yields, scope and the lack of selectivity, are enjoying renewed interest in both academic and industrial laboratories thanks to the use of reactive metal precursors and chelating ligands (Schemes 1.5 and 1.6).[25]

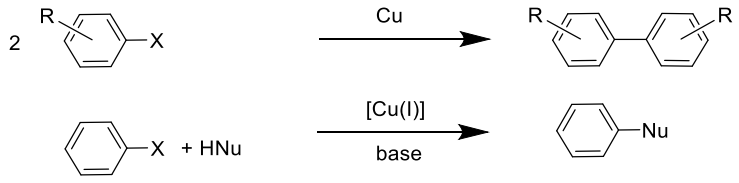

Scheme 1.4: Copper-catalyzed Ullmann reaction (top) and Ullmann-type reactions mediated by Cu(I) complexes (bottom).

CuI CuBr $CuBr{\cdot}SMe_2$ CuCl CuCN Cu_2O
$[Cu(CH_3CN)_4]X$, X = BF_4, PF_6
$Cu_2(OTf)_2{\cdot}$solv, solv = PhH, PhMe

Scheme 1.5: Examples of Cu(I) precursors used for copper-mediated coupling reactions.

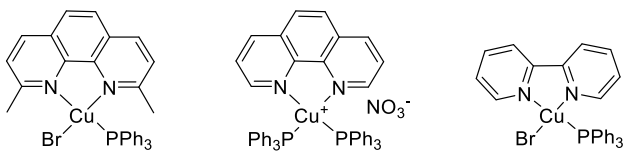

Scheme 1.6: Examples of Cu(I)complexes used in Ullmann-type reactions.[26]

Although only little is known about chemical properties and dynamic behavior of these complexes in solution partly because of possible changes in the coordination number and lability of the Cu(I) center,[27] there are several possible mechanistic pathways leading to Ar-Nu products during Ullmann reactions. The most widely accepted mechanism involves oxidative addition of the halide to Cu^{I}(nucleophile) complex, leading to the formation of a Cu^{III} intermediate (Scheme 1.7a). An alternative explanation (especially for electron-rich ligands) involves single-electron transfer (SET) resulting in the formation of a radical pair (Scheme 1.7b), which can be directly converted into the product or can form a Cu^{III} intermediate after another SET step (Scheme 1.7c). Other possibility, anticipated for electron-poor ligands, includes atom transfer mechanism (Scheme 1.7d), whereas a recent study has suggested that a four-centered σ-bond metathesis mechanism could be the plausible reaction route (Scheme 1.7e).[25]

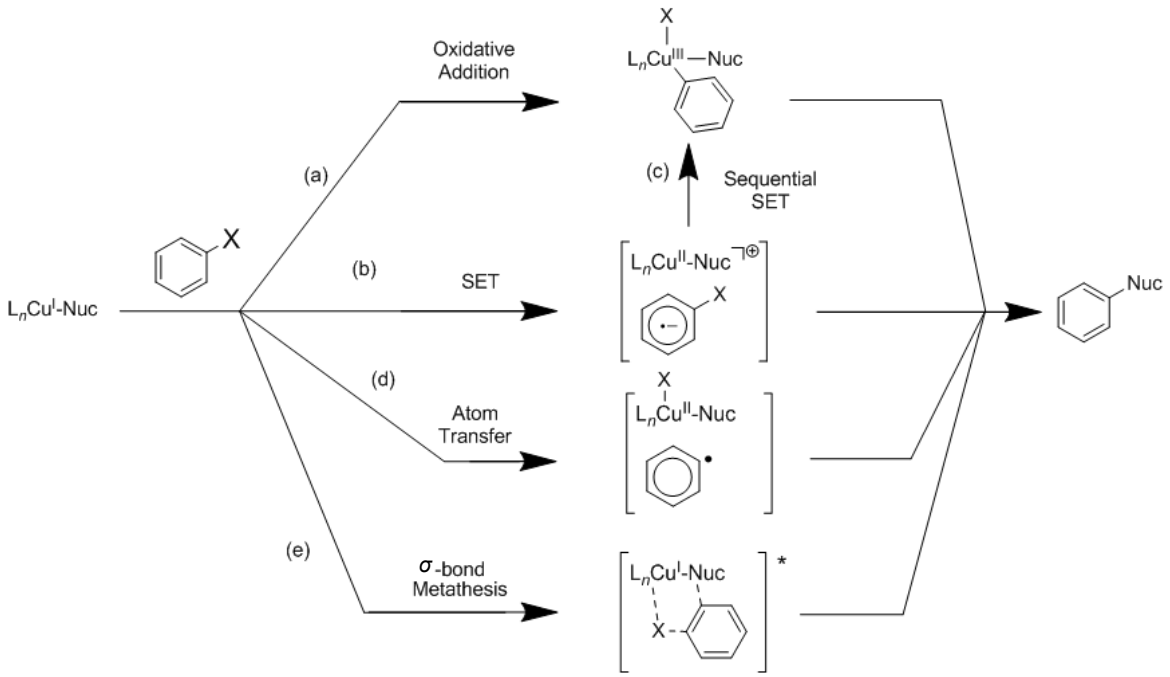

Scheme 1.7: Possible mechanisms of copper-catalyzed Ullmann-type reactions.[25]

In addition to their catalytic use, Cu(I) complexes have attracted attention as promising luminescent materials, largely due to their low cost, interesting phosphorescent properties, diverse structural features, and potential applications in organic light-emitting diodes, photosensitizers, sensing devices, biological imaging and dye-sensitized solar cells.[27] A large

number of mono- and polynuclear Cu(I) complexes have been developed to date and investigated in various applications.[28,29,30]

The recent remarkable progress in the field of Cu(I) luminescent materials has revealed a difference in the photophysical properties of the Cu(I) complexes and those of other noble metal-based luminescent materials. The most distinctive one is the thermally activated delayed fluorescence derived from the small energy difference between the singlet and triplet excited states of Cu(I) as compared to those in noble metal complexes with octahedral and square-planar geometries. Thus, wide modifications in the emission wavelength and the emission lifetime are possible for the luminescent Cu(I) complex systems.[31]

Another attractive research focuses on applications of copper compounds as potential chemotherapeutic agents. Since the serendipitous discovery of cisplatin by Rosenberg et al. in 1965,[32] great efforts have been focused on the anticancer properties of coordination compounds. The cisplatin and its successors, carboplatin and oxaliplatin, are among the most important chemotherapeutics in clinical use worldwide against a variety of different types of cancer (Scheme 1.8). Nevertheless, acquired and intrinsic drug resistance, toxicity and side effects are major drawbacks, which prevent a broader clinical application of these drugs.[33]

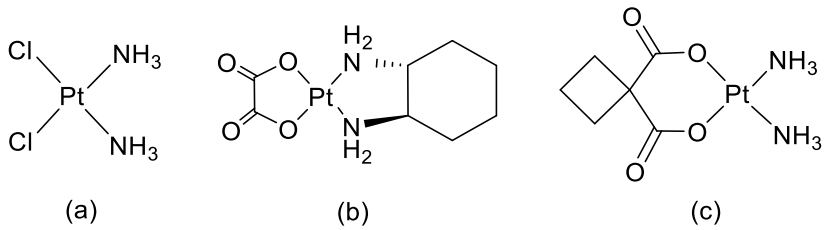

Scheme 1.8: Traditional Pt(II) chemotherapeutics: cisplatin (a), oxaliplatin (b) and carboplatin (c).

Hence, new strategies are being explored to overcome these complications, which include the development of more effective and generally less toxic drugs. In this field, the investigation of copper complexes started with an assumption that endogenous metals may be less toxic than non-essential metal such as platinum for normal cells than cancer cells. Copper is an essential trace element for human life, important for the function of various

enzymes, proteins, DNA synthesis and for regulation of intracellular redox potential. Almost all copper present in the serum of living organisms is bound to ceruloplasmin, the major copper-carrying protein in the blood. Ceruloplasmin binds both copper(I) and copper(II) ions, and brings them to the cell surface. Prior to its uptake into the cell, copper(II) is reduced to copper(I) by metalloreductases at the cell surface. Transport of copper ions through the cell membrane is then mediated by specific transporters.[33,34,35]

Some copper(I) complexes mostly featuring P- and N-donors have been reported to show considerable cytoxic activity (Scheme 1.9). Although the mechanism of their action in tumor cells has not been yet clarified, the reported results suggest that copper(I) complexes are able to overcome cisplatin resistance.[33,36]

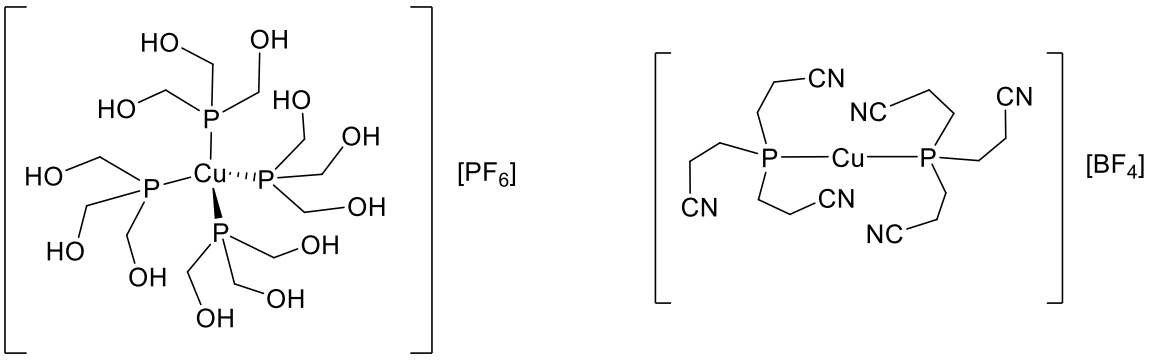

Scheme 1.9: Examples of two phosphine-Cu(I) complexes investigated for anticancer activity.[35]

The Cu(I) complexes are also known for their rich structural chemistry. The diversity of Cu(I) compounds can be illustrated by examining structural chemistry of cuprous halide complexes with ligands such as an aliphatic or aromatic nitrogen heterocycles. Crystallographic studies have demonstrated that complexes of CuI and a particular ligand L form in a variety of structures depending on the stoichiometry (Scheme 1.10). For a 1:1 CuI:L molar ratio, the most commonly encountered motif is the tetranuclear "heterocubane" structure $[Cu_4I_4L_4]$, in which a tetrahedron of copper atoms is embedded within a larger I_4 tetrahedron with each iodide atom residing above a triangular face of the Cu_4 tetrahedron, and the fourth coordination site of each copper is occupied by the additional ligand (L).[37] For CuI:L stoichiometry of 1:2, the most commonly encountered structure is an isolated rhombohedron Cu_2I_2 with alternating copper and halide atoms (for example,

$[CuI(3\text{-picoline})_2]_2$).[38] Compounds of stoichiometry 1:3 have also been reported, being represented by $[CuI(3\text{-picoline})_3]$, which exists as a mononuclear complex with the Cu and I atoms lying on a three-fold axis.[39] In some cases, CuI complexes of the same stoichiometry (e.g., 1:1) exist in more than one stable and crystalline form. For instance, $[Cu_4I_4(py)_4]$ has a cubane form, whereas $[CuI(py)]_n$ is polymeric.[40,30]

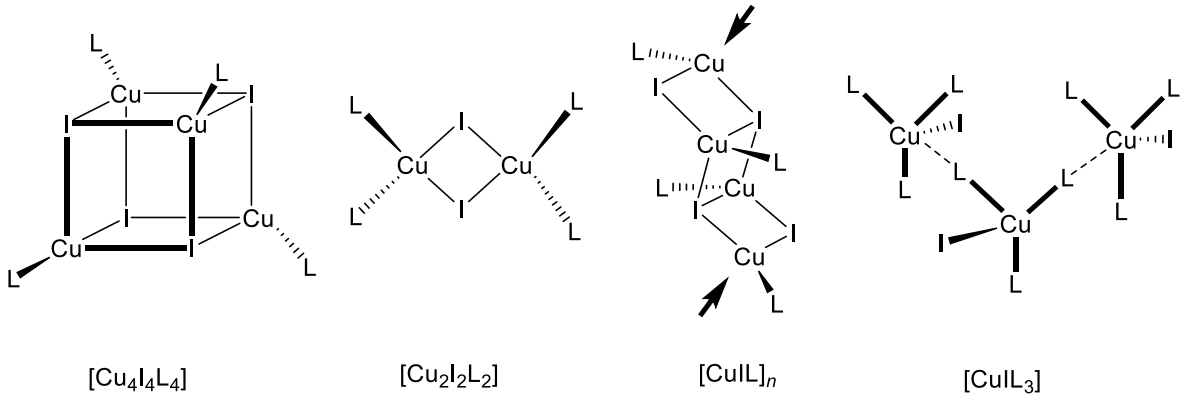

Scheme 1.10: Illustrations of structural diversity of Cu(I) complexes.

Since it has been demonstrated that elimination of a donor from coordination sphere of a metal complex represents an important step in the course of catalytic processes, being associated with the formation of reactive intermediates with possessing an empty coordination site,[41] hemilabile ligands are currently of considerable interest.[42] These polydentate ligands contain at least two electronically different coordination groups (X, Y). Among these, Y represents a substitutionally labile group which can be displaced from the metal center but reactions available for re-coordination, and X is a strongly coordinating group acting as firmly bound pivot (Scheme 1.11).

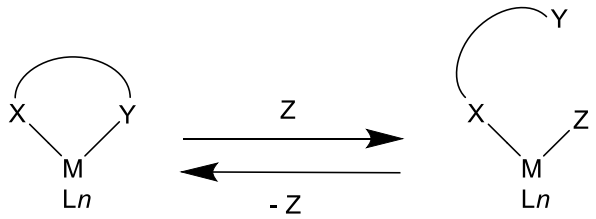

Scheme 1.11: Hemilabile coordination of a bidentate ligand: X = substitutionally inert group, Y = substitutionally labile group, Z = additional ligand, solvent or a substrate in a catalyzed process.

In many syntheses mediated by transition metals, the role of substitutionally inert group is represented by tertiary phosphines (PR_3). Like NH_3, phosphines have a lone pair on the central atom that can be donated to a metal. Similarly to NH_3, however they are also π-acids, to an extent that depends on the nature of R groups in the PR_3 ligand.[43] These neutral ligands are typical soft bases according to the Pearson's HSBA theory and thus form stable complexes with soft acids, such as Rh(I), Ir(I), Pd(II), Cu(I), etc.[44] Phosphines are versatile ligands whose electronic and steric properties can be altered in a systematic and predictable way over a very wide range by changing their substituents (Scheme 1.12). Substitution by groups with a low electronegativity (e.g., alkyl) strengthens σ-donor ability of the phosphorus atom. On the other hand, in the extreme case of PF_3, π-acidity becomes as great as that found for CO. Introduction of bulky substituent increases steric demands of a phosphine donor, which results in an increase in the angles between the substituents, decrease of *s* character of the phosphorus lone pair, and extended phosphorus-metal bond.[45] By using bulky PR_3 ligands, one can favor the formation of low-coordinated metal complexes or can create space for small but weakly binding ligands, which would be excluded by direct competition with smaller ligands such as CO. The usual maximum number of phosphines that can bind to a single metal is two for PCy_3 or $P(i\text{-}Pr)_3$, three or four for PPh_3, four for PMe_2Ph, and five to six for PMe_3.[43]

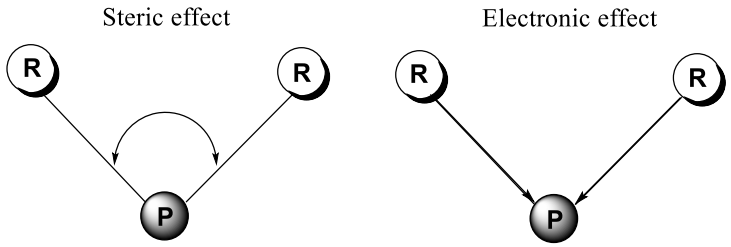

Scheme 1.12: Steric and electronic effect.

The electronic effect of various phosphine ligands can be quantified as suggested Tolman, who compared the *ν*(CO) frequencies of a series of complexes of the type $[(PR_3)Ni(CO)_3]$, containing different PR_3 ligands. Stronger phosphine donors increase the electron density at Ni, which is then relayed further to the CO by back donation. This, in turn, lowers the *ν*(CO) frequencies. Tolman has also quantified the steric effects of phosphines with the so-called cone angle. This is obtained by taking a space-filling model of the $M(PR_3)$ group, folding back the R substituents as far as they will go, and measuring

the angle of the cone that will contain all of the ligand, when the apex of the cone coincides with the metal (Scheme 1.13).[45]

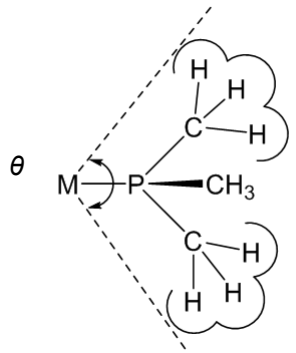

Scheme 1.13: Tolman cone angle *θ*.

Typical examples of hybrid phosphine ligands are ether-phosphines, phosphine-carbonyls and amine-phosphine ligands.[46] In general, the percentage of nitrogen-modified phosphorus ligands studied[47] that exhibit hemilability is not large when compared with the analogous phosphorus-oxygen donors. Interesting class of potentially hemilabile bidentate ligands are also phosphine-nitrile donors. Even though both functional groups (phosphinyl and nitrile) are considered soft donor groups, dative bonding formed by nitrile is usually quite weak. Nitrile group (CN), which is isoelectronic with dinitrogen and carbon monoxide, exerts weak σ-donor and π-acceptor ability and can be readily displaced to afford novel coordination and organometallic complexes.[48] Nitriles can interact with metal centers in several different ways: (a) via simple terminal end-on coordination (η^1-NCR), (b) as side-bonded π-donors (η^2-NCR), and (c) in bridging σ,π-coordination (μ-η^1,η^2-NCR) (Scheme 14). Type (a) is the most common binding mode for nitrile donors, which occurs by σ-coordination trough the nitrogen lone pair.

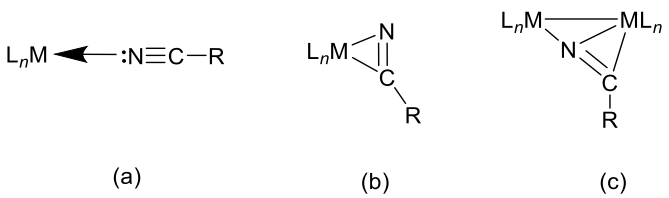

Scheme 1.14: Coordination modes of nitriles: (a) η^1-NCR, (b) η^2-NCR and (c) μ-η^1,η^2-NCR.

Although η^1-coordination is often accompanied by an increase in the *v*(CN) frequency, in several transition metals the value of *v*(CN) has been found unchanged or even lower than for the respective free ligands. This has been ascribed to significant "back bonding" between the metal *d* orbitals and π^* orbitals of the nitrile groups in these compounds.[48]

In the majority of coordination compounds featuring simple phosphinonitrile donors, such as Ph_2PCH_2CN,[49] $(Ph_2P)_2CHCN$,[50] and $Ph_2PCH(CN)_2$[51], these ligands coordinate as simple P-donors, with their cyano groups acting as auxiliary substituents. Compounds in which both functional groups are coordinated to a metal centre remain extremely rare and have not been unequivocally confirmed, by using methods of direct structural analysis until recently (see below).[52]

In 1972, coordination compounds with 2-(diphenylphosphino)benzonitrile (**L°**) of the type $[M(CO)_3(\mathbf{L^o})X]_y$, where M is group VII metal, were prepared and studied. Their infrared spectra were consistent with coordination of both the phosphorus atom and the CN bond (Scheme 1.15).[53]

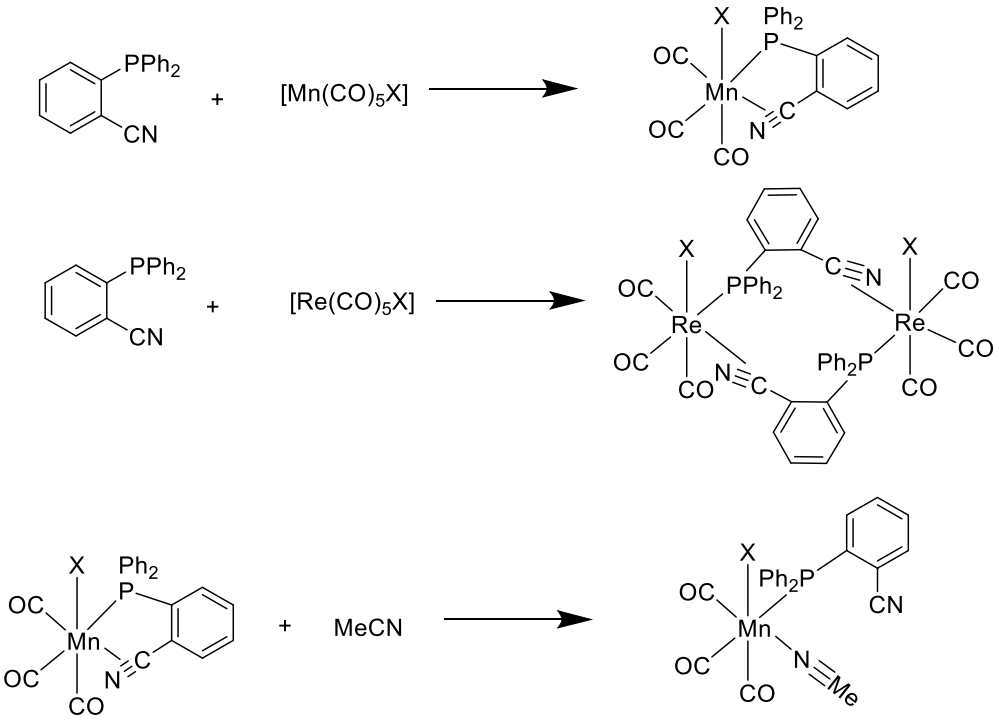

Scheme 1.15: The first examples of complexes featuring P,N-coordinated phosphinonitrile ligands.

The same ligand, 2-(diphenylphosphino)benzonitrile (**L°**), was also used to prepare a trimeric P,CN-bridged triplatinum(II) complex (Scheme 1.16).[54]

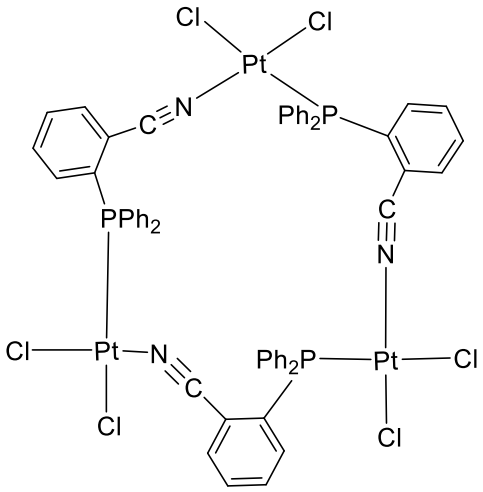

Scheme 1.16: Trimeric complex $[PtCl_2(\mathbf{L^o})]_3$.

Recently, our research group published a series of Au(I), Ag(I) and Cu(I) complexes with 1'-(diphenylphosphino)-1-cyanoferrocene (Scheme 1.17). [52,55,56]

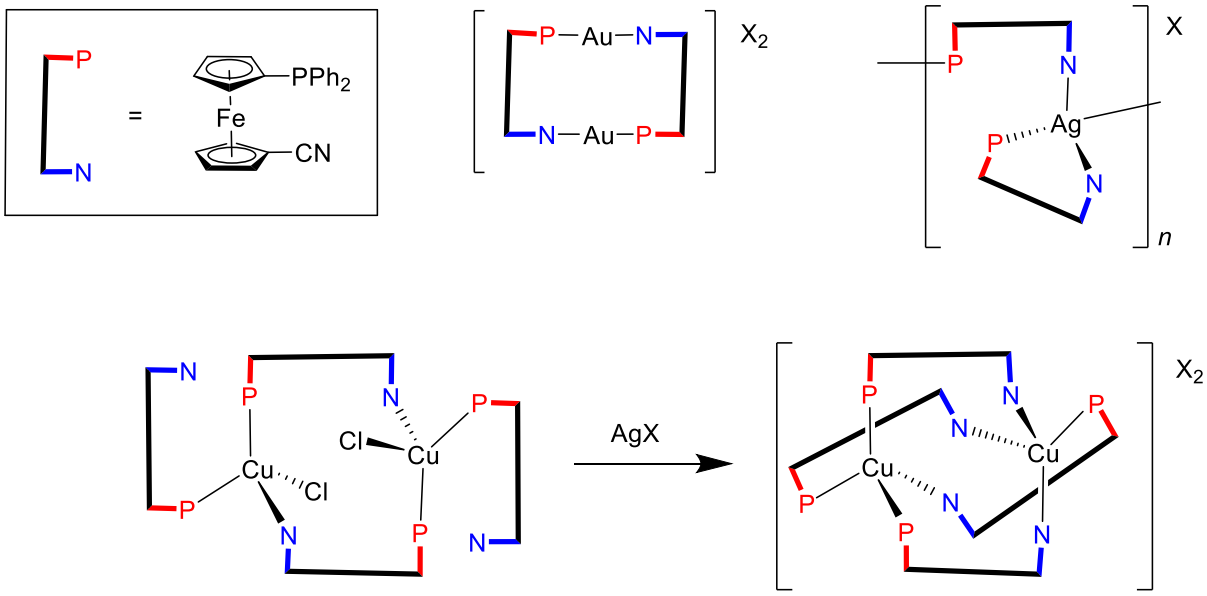

Scheme 1.17: Selected complexes with 1'-(diphenylphosphino)-1-cyanoferrocene.

For the first case, it was unequivocally demonstrated that phosphinonitrile donors can coordinate as P,N-bridges through both soft donor sites. The preparation and study of new phosphinonitrile complexes are the main aims of this work.

1.1 Aims of the Thesis

The aim of this Thesis was to prepare and study copper(I) complexes containing two isomeric phosphinonitrile donors, namely 2-(diphenylphosphino)benzonitrile (**L^{o}**) and 4-(diphenyl-phosphino)benzonitrile (**L^{p}**). Main emphasis was put on finding new structural motifs and differences in coordination behavior of these hybrid ligands. As a Cu(I) source, all commonly accessible copper(I) compounds such as halides CuX (X = Cl, Br, I), pseudohalides (X = CN, SCN), and ionic precursors such as tetrakis(acetonitril)copper(I) tetrafluoroborate, $[Cu(MeCN)_4][BF_4]$, were used.

All prepared compounds were characterized by nuclear magnetic resonance and infrared spectroscopy, by elemental analysis, mass spectrometry, and their solid-state structures were determined by single-crystal X-ray diffraction analysis. In addition, luminescent properties of the isolated Cu(I) complexes were studied and catalytic activity of the selected representatives was studied in copper-catalyzed alkyne-azide cycloaddition (CuAAC) leading to 1,2,3-triazoles.

2. Results and discussion

2.1 Phosphinonitrile donors

Phosphinonitrile Cu(I) complexes reported in this Thesis contain two known isomeric ligands, viz. 2-(diphenylphosphino)benzonitrile (**L^o**)[57,54,58] and 4-(diphenylphosphino)benzonitrile (**L^p**),[57,59,60] which can both be regarded functional derivatives of the ubiquitous triphenylphosphine (Scheme 2.1). Different spatial distribution of the donor groups in **L^o** and **L^p** obviously leads to different coordination behavior. Thus, ligand **L^p** can be expected to coordinate metal ions only via the phosphine group (**L^p**-*κP*) or form bridges (μ(P,N)-**L^p**) between two metal atoms. In contrast, the mutual orientation of nitrile and phosphine groups in **L^o** can allow for chelate coordination to one metal atom (**L^o**-κ^2*P*,*N*), although the nature of the nitrile group, mostly its rod-like geometry and rigidity, disfavors this coordination mode.

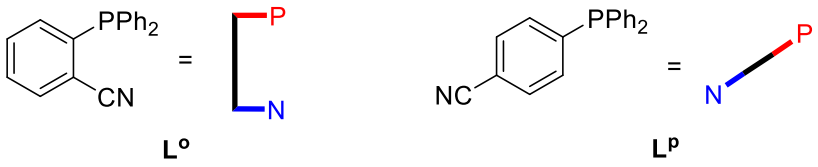

Scheme 2.1: The studied isomeric phosphinonitrile ligands.

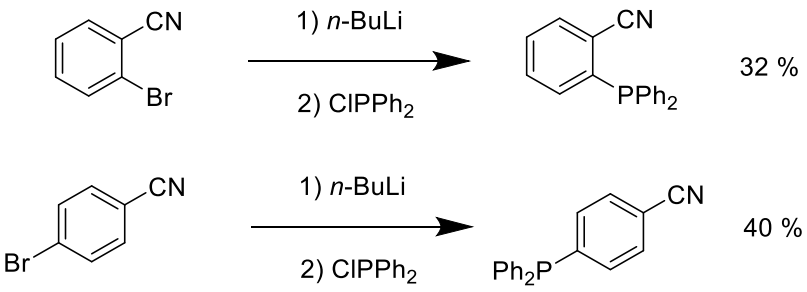

Scheme 2.2: Synthesis of phosphinonitrile ligands **L^o** and **L^p**.

Ligands **L^o** and **L^p** donors were prepared by using organolithium reagents according to the literature (Scheme 2.2).[58,60] **L^p** is described in the literature as a pale yellow solid.[60] We

obtained a product which showed an intense yellow luminescence caused by an unidentified trace impurity, which could not be removed by chromatography. Fortunately, the impurity could be removed by addition of charcoal to a solution of **L^{p}** in hot heptane. Subsequent filtration and crystallization by cooling afforded analytically pure **L^{p}** as a white microcrystalline product.

The structure of **L^{o}** had been determined before.[61] However, to the best of our knowledge, the structure of **L^{p}** has not yet been published. We obtained a single-crystal of this compound suitable for X-ray analysis by slow cooling of its solution in hot heptane to −20 °C (Figure 2.1).

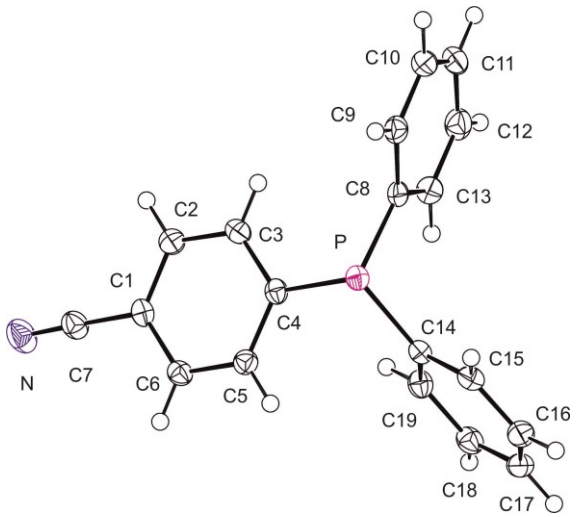

Figure 2.1: Molecular structure of ligand **L^{p}**. Displacement ellipsoids are shown at the 50% probability level.

Ligand **L^{o}** crystallizes[61] with the symmetry of the triclinic space group $P\bar{1}$ and two formula units per the unit cell. On the other hand, ligand **L^{p}** crystallizes with the symmetry of the monoclinic space group $P2_1/n$ and four formula units in the unit cell. Selected structural parameters for both ligands are shown in Table 2.1. Crystallographic data are presented in Table 5.1.

Table 2.1: Selected geometric data for phosphinonitrile ligands **L^p** and **L^o** (in Å and °).[61]

Parametr	**L^p**	**L^o**
N-C7	1.148(2)	1.141(1)
P-C14	1.839(2)	1.833(2)
P-C8	1.834(2)	1.830(2)
P-C4	1.834(2)	1.838(2)

Parametr	**L^p**	**L^o**
C1-C7-N	178.7(2)	179.0(2)
C4-P-C8	101.4(1)	103.5(1)
C8-P-C14	103.8(1)	103.5(2)
C4-P-C14	102.7(1)	101.0(1)
C6-C1-C7	119.2(2)	119.7(2)
C2-C1-C7	120.7(2)	118.5(2)
P-C4-C5	119.6(1)	117.7(2)
P-C4-C3	121.6(2)	124.9(2)

2.2 Synthesis of Cu(I) complexes

Several copper(I) compounds were utilized as a source of the Cu(I) ions. Namely, copper(I) halides CuX (X = Cl, Br, I), selected pseudohalides (X = CN, SCN) and tetrakis(acetonitrile)copper(I) tetrafluoroborate. All complexation reactions were performed at the 1:1 and 1:2 metal-to-ligand ratios.

The preparation of the complexes was typically accomplished by simple mixing of the respective ligand with the selected Cu(I) precursor at the given stoichiometry ratio in a polar solvent (CH_2Cl_2, MeOH or their mixture). After stirring (typically for 2 h), the solvent was evaporated, the solid residue was dissolved in a small amount of a suitable solvent, and the resulting solution was filtered and layered by a non-polar solvent to induce crystallization.

Complexes containing L^o

All six Cu-halide complexes containing **L^o** donor, compound **1**, **2**, **3**, and **4a-c**, were successfully crystallized and structurally characterized (Table 2.2). In their structures, four different coordination modes were detected. The reaction of CuCl with **L^o** at the 1:1 molar ratio surprisingly yielded a product with Cu:**L^o** composition of 4:3, complex **1**. On the other

hand, crystallization of the solid obtained by the reaction of CuI and **L^o** at the same ratio led to a product with 3:2 stoichiometry (Cu:**L^o**), complex **3**. The Cu:**L^o** molar ratios in other halide complexes (compounds **2** and **4a-c**) corresponded with the reaction stoichiometry (Scheme 2.3).

Reaction of copper(I) cyanide and **L^o** at both tested ratios (i.e., at 1:1 and 1:2 CuCN:**L^o** ratios) produced the same crystalline product with 1:1 metal-to-ligand stoichiometry (Scheme 2.3, compound **7**). Direct reaction of copper(I) thiocyanate with **L^o** led to a white precipitate, which proved to be insoluble in all common solvents (CH_2Cl_2, MeOH, EtOH, MeCN,...). It was thus impossible to prepare a defined crystalline product (even by reactive diffusion approach), and the product of this reaction could not be adequately characterized.

Table 2.2: Summary of tested coordination reactions with ligand **L^o** and the isolated complexes.

Reaction	Cu:L ratio	Product	Compound Number
CuCl + **L^o**	1:1	$[Cu_4Cl_4(\mathbf{L^o})_3]$	**1**
CuCl + **L^o**	1:2	$[CuCl(\mathbf{L^o})_2]$	**4a**
$CuBr{\cdot}SMe_2$ + **L^o**	1:1	$[Cu_4Br_4(\mathbf{L^o})_4]$	**2**
$CuBr{\cdot}SMe_2$ + **L^o**	1:2	$[CuBr(\mathbf{L^o})_2]$	**4b**
CuI + **L^o**	1:1	$[CuI(\mathbf{L^o}){\cdot}CuI{\cdot}CuI(\mathbf{L^o}){\cdot}2CHCl_3]_n$	**3**
CuI + **L^o**	1:2	$[CuI(\mathbf{L^o})_2]$	**4c**
CuCN + **L^o**	1:1	$[CuCN(\mathbf{L^o})]_n$	**7**
CuCN + **L^o**	1:2	$[CuCN(\mathbf{L^o})]_n$	**7**
CuSCN + **L^o**	1:1	unknown insoluble product	-
CuSCN + **L^o**	1:2	unknown insoluble product	-
$[Cu(MeCN)_4][BF_4]$ + **L^o**	1:1	$[Cu_2(MeCN)_2(H_2O)_2(\mathbf{L^o})_2][BF_4]_2$	**8**
$[Cu(MeCN)_4][BF_4]$ + **L^o**	1:2	$[Cu_3(\mathbf{L^o})_6][BF_4]_3{\cdot}CH_2Cl_2$ $[Cu(\mathbf{L^o})(\mathbf{L^o}OMe)]_2[BF_4]_2{\cdot}6CHCl_3$	**9** **10**

Reactions of tetrakis(acetonitrile)copper(I) tetrafluoroborate with **L^o** led to three quite unexpected products (Table 2.2). The reaction performed at the ratio of 1:1 afforded a dinuclear product which contained μ(P,N)-bridging **L^o**, acetonitrile and water as the ligands

(Scheme 2.3, compound **8**). The product of the reaction performed at the Cu:**L^o** ratio 1:2 furnished a mixture of trimeric complex $[Cu_3(\mathbf{L}^o)_6][BF_4]_3$ and another product, in which one of the nitrile groups reacted with the methanol used as solvent to form a phosphino-imidate ligand (Scheme 2.3, compounds **9** and **10**). Experiments aimed at the preparation of a complex featuring two ligands with imidate groups failed (lengthening of the reaction time, refluxing of the complex in methanol). Although unable to isolate this complex, we observed peaks corresponding to $[Cu(\mathbf{L}^o OMe)_2]^+$ cations in ESI mass spectrum of complex **10**.

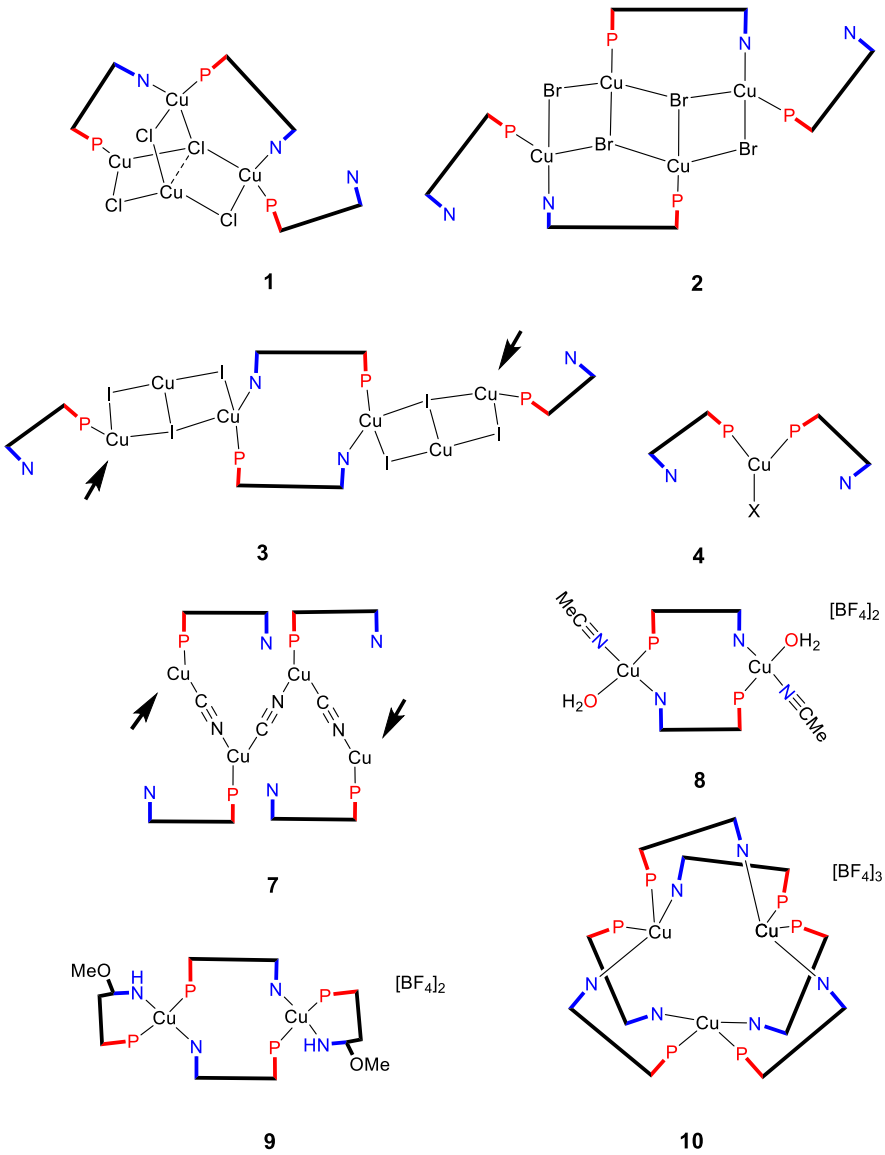

Scheme 2.3: Schematic depiction of the structures of complexes containing **L^o**. The arrows indicate the propagation of the polymeric chains.

Complexes containing $\mathbf{L^p}$

Experiments with ligand $\mathbf{L^p}$ proved to be significantly less fruitful (Table 2.3). For instance, the reactions of copper(I) chloride and copper(I) bromide at the 1:1 molar ratio resulted in polymeric complexes **5** (Scheme 2.4). On the other hand, copper(I) iodide, and in a negligible extent also copper(I) bromide, furnished heterocubanes **6** (Scheme 2.4). Analogous reactions at the 1:2 molar ratio gave solid products which defied all attempts of crystallization, separating as oily intractable materials. Hence, these compounds were not studied further.

Table 2.3: Summary of tested coordination reactions with ligand $\mathbf{L^p}$ and the prepared complexes.

Reaction	Cu:L ratio	Product	Compound Number
CuCl + $\mathbf{L^p}$	1:1	$[CuCl(\mathbf{L^p})\cdot 2CHCl_3]_n$	**5a**
CuCl + $\mathbf{L^p}$	1:2	non-crystalline material	-
$CuBr\cdot SMe_2$ + $\mathbf{L^p}$	1:1	$[CuBr(\mathbf{L^p})\cdot 0.5CH_2Cl_2]_n$ $[CuBr(\mathbf{L^p})]_4\cdot CH_2Cl_2$	**5b** **6b**
$CuBr\cdot SMe_2$ + $\mathbf{L^p}$	1:2	non-crystalline material	-
CuI + $\mathbf{L^p}$	1:1	$[CuI(\mathbf{L^p})]_4$	**6c**
CuI + $\mathbf{L^p}$	1:2	non-crystalline material	-
CuCN + $\mathbf{L^p}$	1:1	unknown insoluble product	-
CuCN + $\mathbf{L^p}$	1:2	unknown insoluble product	-
CuSCN + $\mathbf{L^p}$	1:1	unknown insoluble product	-
CuSCN + $\mathbf{L^p}$	1:2	unknown insoluble product	-
$[Cu(MeCN)_4][BF_4]$ + $\mathbf{L^p}$	1:1	unknown insoluble product	-
$[Cu(MeCN)_4][BF_4]$ + $\mathbf{L^p}$	1:2	unknown insoluble product	-

In the case of reactions with pseudohalides, the products were obtained in the form of insoluble precipitates. This is probably due to a poor solubility of Cu(I) pseudohalides themselves, or a possible formation of coordination polymers. Insoluble products resulted also from the reactions of $\mathbf{L^p}$ with tetrakis(acetonitrile)copper(I) tetrafluoroborate (at both molar ratios). Repeated attempts to obtain defined crystalline products by reactive diffusion failed.

In addition, the reactions of tetrakis(acetonitrile)copper(I) tetrafluoroborate with both ligands **L^{o}** and **L^{p}** (ratio 1:1) were studied. During these studies it was found that irrespective of the order of the addition of the ligands, an insoluble product is formed once ligand **L^{p}** is added to the reaction mixture.

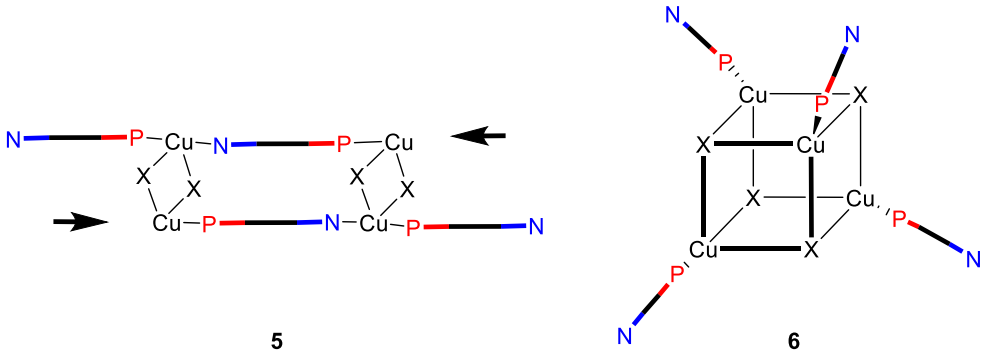

Scheme 2.4: Schematic depiction of the structures of complexes containing **L^{p}**. The arrows indicate propagation of polymeric chain.

2.3 X-ray diffraction analysis

The crystal structures of compounds **1**-**10** were determined by single-crystal X-ray diffraction analysis. Selected crystallographic data for all complexes are presented in Attachments.

The structure of [(μ-Cl)$_3$(μ$_3$-Cl)Cu$_4$(L^{o}-κ*P*){μ(P,N)-L^{o}}$_2$] (1)

Colorless crystals of complex **1** were grown by liquid-phase diffusion of hexane into a solution of this complex in methanol/dichloromethane (1:1). The compound crystallizes in triclinic crystal system with the symmetry of the $P\bar{1}$ space group and two formula units per the unit cell. The compound **1** as seen in this crystal structure is depicted in Figure 2.2.

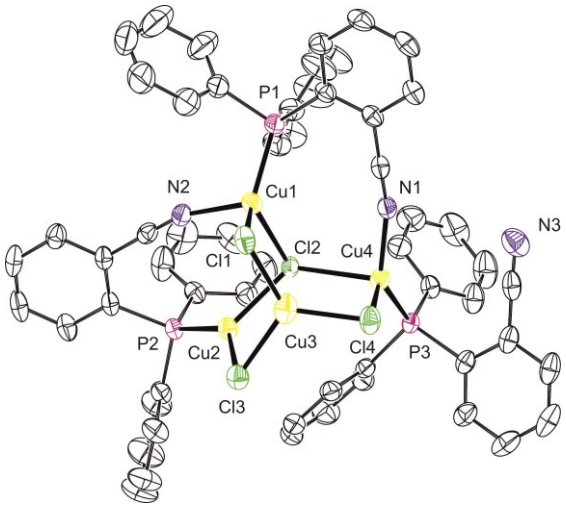

Figure 2.2: Molecular structure of **1**. Displacement ellipsoids correspond to the 50% probability level. All hydrogen atoms are omitted for clarity.

X-ray analysis of **1** reveals a tetranuclear structure with two tetrahedrally (Cu1 and Cu4) and two trigonally (Cu2 and Cu3) coordinated copper(I) atoms, which are all non-equivalent (Scheme 2.5). Both tetrahedrally coordinated copper atoms are surrounded by two chloride ions, one phosphine and one nitrile group. The Cu2 atom binds phosphine group and two chloride ions, whereas the Cu3 atom coordinates only three chloride ions with an average Cu-Cl distance of 2.28 Å. The distance of Cu3 to Cl2 of 2.940(1) Å suggests a possible weaker supporting interaction and can lead to tetrahedral geometry around Cu3. The complex contains two ligands **L^o**, whose both functional groups are coordinated, and one **L^o** ligand that binds as a simple P-donor, with its nitrile group acting as an auxiliary substituent. Selected interatomic distances and angles are presented in Table 2.4. A similar type of structure was already observed in a complex containing trimethylphosphine.[62]

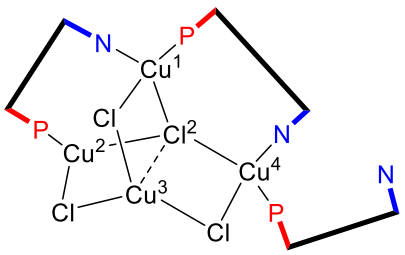

Scheme 2.5: The structure of $[Cu_4Cl_4(\mathbf{L^o})_3]$ (**1**).

Table 2.4: Selected data for complex **1** (in Å and °).

Cu1-Cl1	2.315(1)	Cu1-P1	2.201(1)
Cu1-Cl2	2.415(1)	Cu2-P2	2.188(1)
Cu2-Cl2	2.319(1)	Cu4-P4	2.197(1)
Cu2-Cl3	2.243(1)	Cu1-N2	2.061(2)
Cu3-Cl1	2.248(1)	Cu4-N1	1.965(2)
Cu3-Cl2	2.940(1)	C1-N1-Cu4	165.0(2)
Cu3-Cl3	2.332(1)	C2-N2-Cu1	163.1(1)
Cu3-Cl4	2.245(1)	Cl2-Cu4-Cl4	103.1(1)
Cu4-Cl2	2.507(1)	Cl2-Cu2-Cl3	111.4(1)
Cu4-Cl4	2.335(1)	Cl1-Cu1-Cl2	105.1(1)
		Cl3-Cu3-Cl4	116.9(1)

The structure of $[(\mu\text{-Br})_2(\mu_3\text{-Br})_2Cu_4(L^o\text{-}\kappa P)_2\{\mu(P,N)\text{-}L^o\}_2]$ (2)

Yellow crystals of **2** suitable for X-ray diffraction analysis were grown by liquid-phase diffusion of hexane into a solution of **2** in 1,2-dichloroethane. The compound crystallizes in triclinic crystal system with the symmetry of the $P\bar{1}$ space group and one formula unit in the unit cell. The molecular structure of compound **2** is shown in Figure 2.3.

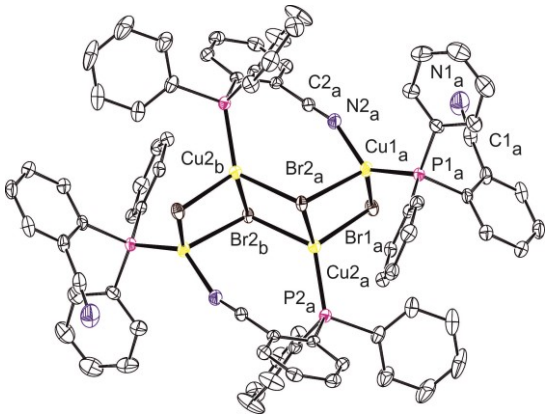

Figure 2.3: Molecular structure of **2**. Displacement ellipsoids are scaled to the 50% probability level. Hydrogen atoms are omitted.

The structure of **2** can be described as a tetranuclear „open heterocubane". Of the four **L°** ligands, two employ both functional groups in coordination and two coordinate as P-monodentate donors. All copper atoms are tetrahedrally coordinated while the bromide ions occur in the form of μ-Br or μ_3-Br bridges (Scheme 2.6).

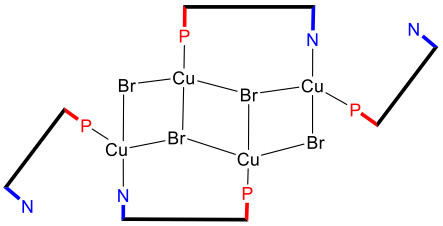

Scheme 2.6: The structure of **2**.

Among the form Cu_2Br_2 squares, the longest Cu-Br bond is associated with Cu1a and Br2a (2.602(1) Å), and the shortest one with atoms Cu1a and Br1a (2.486(1) Å). The smallest angle in the squares represents the Cu2a-Br2a-Cu1 angle (74.08(1)˚), and the most opened is the Br2a-Cu1a-Br1 angle (103.8(1)˚). Selected interatomic distances and angles are presented in Table 2.5 and correspond with an analogous complex containing triphenylphosphine.[63]

Table 2.5: Selected data for complex **2** (in Å and ˚).

Cu1a-P1a	2.210(1)	N1a-C1a	1.143(1)
Cu2a-P2a	2.228(1)	Cu2b-Br2a	2.529(1)
Cu1a-Br1a	2.486(1)	Cu2a-Br1a-Cu1a	78.0(1)
Cu1a-Br2a	2.602(1)	Cu2a-Br2a-Cu1a	74.08(1)
Cu2a-Br1a	2.494(3)	Br2a-Cu1a-Br1a	103.8(1)
Cu2a-Br2a	2.494(1)	Br2a-Cu2a-Br1a	103.7(1)
Cu1a-N2a	1.988(2)	Br2a-Cu2a-Br2b	89.0(1)
N2a-C2a	1.143(1)		

The structure of $[(\mu_3\text{-I})Cu(\mu_2\text{-I})_2Cu_2\{\mu(P,N)\text{-L}^o\}_2]_n$ (3)

Yellow-white crystals of **3** used for X-ray diffraction analysis experiment were obtained by liquid-phase diffusion of hexane into a solution of **3** in chloroform. The

compound crystallizes as a stoichiometric solvate **3**·2$CHCl_3$ in the monoclinic crystal system with the symmetry of the *C*2/*c* space group and four formula units for the unit cell. Molecular structure of this coordination polymer is shown in Figure 4. Selected interatomic distances and angles are collected in Table 2.6.

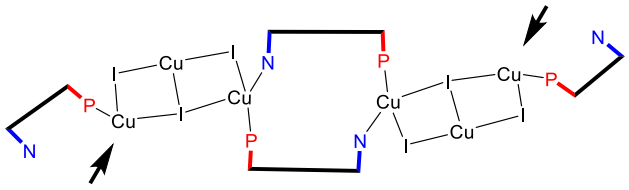

Scheme 2.7: The structure of **3**. The arrows indicate propagation of the polymeric chain.

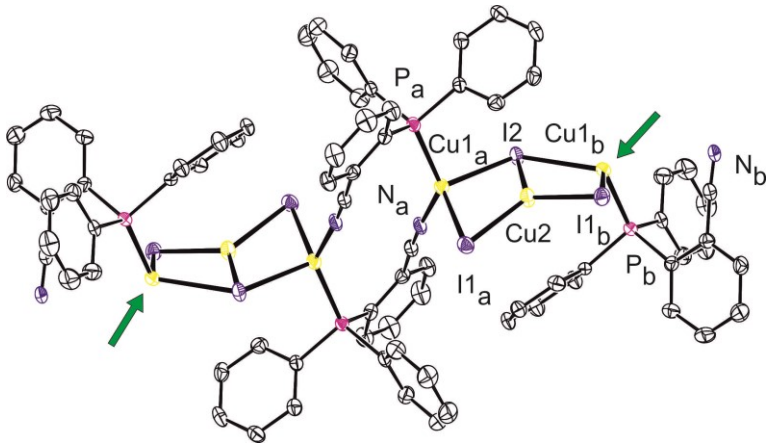

Figure 2.4: Structure of polymer **3**. Arrows symbolize the direction of other bonds. Displacement ellipsoids are shown at the 50% probability level. For clarity, all hydrogen atoms are omitted.

The structure of **3** reveals polymeric complex comprising trigonally (Cu2) and tetrahedrally (Cu1) coordinated copper atoms (Scheme 2.7). Distorted trigonal I_3 environment around the copper Cu2 ion contains two equivalent and one unique Cu-I bonds (2.762(1) Å, 2.567(1) Å). Each of the tetrahedrally copper ions are coordinated by two iodide ions and two **L°** ligands (one through the phosphorus and one through its CN group) which interconnect the trimeric Cu_3I_3 units into an infinite one-dimensional chain. The iodide ions bind as μ-I or μ_3-I bridges. The smallest angle in the Cu_2I_2 square represents the Cu1-I2-Cu2 angle (60.4(1)˚) and the most opened is the Cu1-I2-Cu2 angle (111.6(1)˚). Two structurally equivalent squares are mutually tilted as evidenced by the I1a-Cu2-I1b angle

of 112.0(1)˚. Additional interatomic distances and angles are presented in Table 2.6. Similar structure motive was observed in the molecular complex featuring 2,5-bis[(diphenyl-phosphino)-methyl]thiophene.[64]

Table 2.6: Selected data for complex **3** (in Å and ˚).

Cu1a-P1a	2.232(1)	Cu1-I1-Cu2	60.9(1)
N-Cu1a	1.958(1)	Cu1-I2-Cu2	60.4(1)
Cu1a-I1a	2.718(1)	Cu1-I2-Cu1a	120.7(1)
Cu2-I1a	2.567(1)	I1a-Cu2-I1b	112.0(1)
Cu2-I2	2.565(1)	Cu-N-C	174.0(1)
Cu1a-I2	2.762(1)	C-C-N	176.6(1)
N-C	1.140(1)		

The structures of [CuX(L^{o}-κ*P*)$_2$] (4a-c)

Colorless crystals of **4a** were grown by liquid-phase diffusion of hexane into a solution of this complex in ethyl acetate. The compound crystallizes in monoclinic crystal system with the symmetry of the *C*2/*c* space group and four units per the unit cell. The compound **4a** as seen in this crystal structure is depicted in Figure 2.5. Colorless crystals of **4b** suitable for X-ray diffraction analysis were obtained similarly. However, the compound crystallizes in triclinic crystal system with the symmetry of the $P\bar{1}$ space group and two units in the unit cell. The molecular structure of **4b** is shown in Figure 2.6. Finally, colorless crystals of **4c** used for X-ray diffraction analysis experiment were obtained by liquid-phase diffusion of hexane into a solution of **4c** in chloroform. The compound crystallizes in monoclinic crystal system with the symmetry of the *C*2/*c* space group and four units per the unit cell. Molecular structure of this complex molecule is shown in Figure 2.7.

Compounds **4a-c** can be described as mononuclear complexes with trigonally coordinated metal centers. The copper(I) atoms have similar distorted XP_2 coordination environments and the phosphinonitrile ligands coordinate only as P-monodentate donors. In the case of **4a** and **4c**, both **L^{o}** ligands are symmetrically equivalent. The Cu-P bond lengths in these complexes are very similar, differing only at the second decimal place (average value 2.242 Å). However, a substantial variation is observed for the P-Cu-P angles (142.2(1)˚

for **4a**, 123.9(1)˚ for **4b**, and 123.2(1)˚ for **4c**). Selected interatomic distances and angles are presented in Table 2.7 and are in agreement with reported values for similar compounds.[65,66,67]

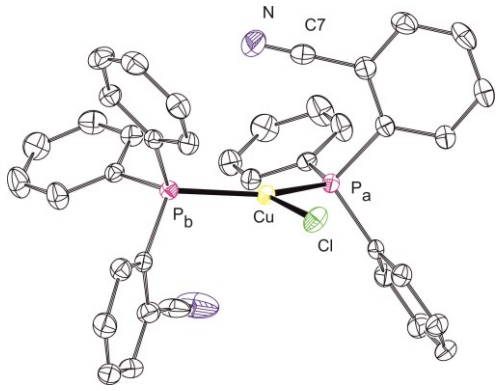

Figure 2.5: Molecular structure of **4a**. Displacement ellipsoids are shown at the 50% probability level. The hydrogen atoms are omitted to avoid complicating the figure.

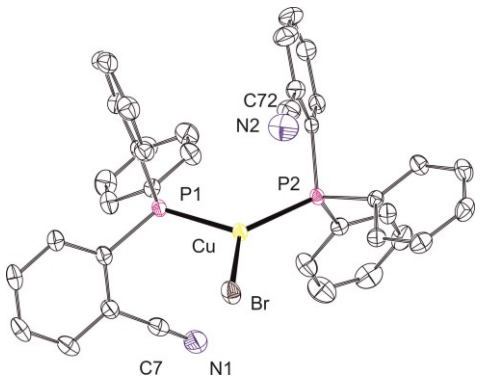

Figure 2.6: Molecular structure of **4b**. Displacement ellipsoids are scaled to the 50% probability level. Hydrogen atoms are omitted.

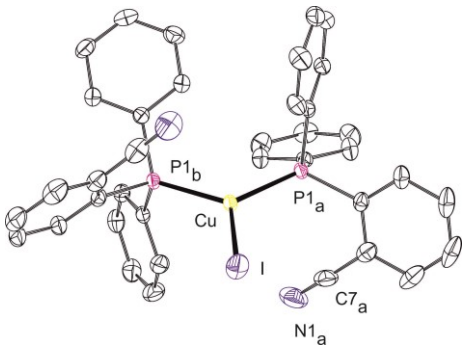

Figure 2.7: Molecular structure of **4c**. Displacement ellipsoids enclose at the 50% probability level. The hydrogen atoms are not shown.

Table 2.7: Selected geometric data for complexes **4a-c** (in Å and °).

	4a	**4b**	**4c**
Cu-P1	2.238(1)	2.253(1)	2.244(1)
Cu-P2	-	2.234(1)	-
Cu-X	2.251(1)	2.334(1)	2.490(1)
N1-C7	1.141(1)	1.141(3)	1.142(3)
N2-C2	-	1.142(3)	-
P-C14	1.823(2)	1.827(2)	1.1824(2)
P-C14	1.826(2)	1.8212(2)	1.822(2)
P-C4	1.837(2)	1.832(2)	1.836(2)

	4a	**4b**	**4c**
P1-Cu-P2	142.2(1)	123.9(1)	123.2(1)
P1-Cu-X	108.9(1)	111.0(1)	118.5(1)
P2-Cu-X	-	124.9(1)	-
C1-C7-N1	177.6(1)	178.6(2)	177.9(2)
C1-C7-N2	-	177.8(2)	-

The structures of $[\{\mu(P,N)\text{-}L^o\}Cu(\mu_2\text{-}X)]_n$ (5a and 5b)

Yellow crystals of complex **5a** were grown by liquid-phase diffusion of hexane into a solution of this complex in chloroform. The compound crystallizes as solvate **5a**·2$CHCl_3$ in monoclinic crystal system with the symmetry of the *P*21/*n* space group. The molecular structure of **5a** is shown in Figure 2.8. Yellow crystals of **5b** used for X-ray diffraction analysis experiment were obtained by liquid-phase diffusion of hexane into a solution of **5b** in dichloromethane. The compound crystallizes as solvate **5b**·0.5CH_2Cl_2 in triclinic crystal system with the symmetry of the space group $P\bar{1}$. The complex molecule in the structure of **5b**·0.5CH_2Cl_2 is disordered. The Cu_2Br_2 units occupy two positions. The structure depicted in Figure 2.9 shows the major contributing moiety (occupancy 94.8(1)%).

Table 2.8: Selected data for complex **5a** (in Å and °).

Cu-Cl	2.387(2)
Cu-Clc	2.392(2)
Cu-P	2.203(1)
Cu-Nb	1.959(3)
Nb-C7b	1.145(5)
Cu-Cuc	3.081(1)
Cl-Clc	3.654(2)

Cl-Cu-Clc	99.7(1)
Cu-Cl-Cuc	80.3(1)
P-Cu-Nb	122.7(2)
P-Cu-Cl	108.3(4)
P-Cu-Clc	110.4(1)
Cu-Nb-C7b	174.0(3)
Nb-C7b-C4b	177.2(4)

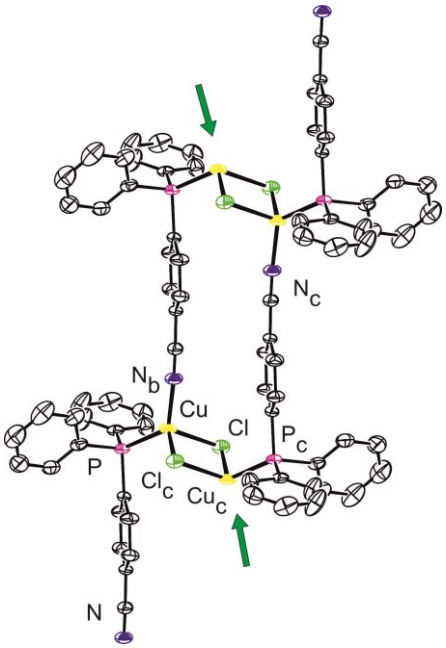

Figure 2.8: Molecular structure of **5a**. Displacement ellipsoids are shown at the 50% probability level. The arrows indicate propagation of the polymeric chain. Hydrogen atoms are not shown.

Table 2.9: Selected data for complex **5b** (in Å and ˚).

Cu1-Br1	2.480(1)	N1-Cu1-Br1	109.0(2)
Cu1-Br1c	2.515(1)	N1-Cu1-Br1c	103.0(2)
Cu1-Cu1c	3.037(2)	Br1-Cu1-Br1c	105.1(1)
Cu1-N1	1.973(3)	Cu1-Br1-Cu1c	74.9(1)
Cu1-P1b	2.214(1)	Cu1-N1-Cu7	175.0(3)
N1-C7	1.148(4)	N1-Cu1-P1b	117.8(1)
		P1b-Cu1-Br1c	111.4(1)
		P1-Cu1-Br1c	109.8(1)

Each copper(I) ion in the structure of **7** and **8** is coordinated by two $\mathbf{L}^{\mathbf{p}}$ ligands (one through the phosphorus and one through its CN group), and the resulting Cu($\mathbf{L}^{\mathbf{p}}$)$_2$ units are connected into dimeric moieties by a pair of asymmetric halide bridges [Δ(Cu-X) $\approx$ 0.04 Å] that complete the distorted tetrahedral coordination spheres around the Cu(I) ions. Because each ligand acts as P,N bridge between two adjacent dicopper(I) units, the dimer units are interlinked into infinite chains. Similar types of these polymeric complexes were prepared

by the reaction of copper(I) halides with 1'-(diphenylphosphino)-1-cyanoferrocene.[52] Selected interatomic distances and angles are presented in Tables 2.8 and 2.9.

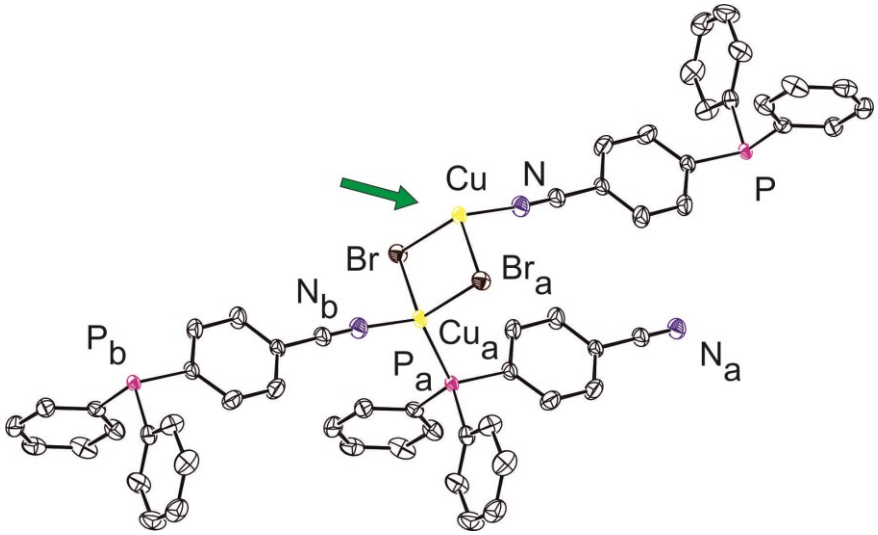

Figure 2.9: Molecular structure of **5b**. Displacement ellipsoids are shown at the 50% probability level. The arrows indicate propagation of polymeric chain. Note: only the major contributing disordered Cu and Br ions are shown and all hydrogen atoms are omitted.

The structures of heterocubanes [(μ$_3$-X)$_4${Cu(L^o-κ*P*)}$_4$] (6b and 6c)

Colorless crystals of **6b** used for X-ray diffraction analysis experiment were obtained by liquid-phase diffusion of hexane into a solution of **6b** in dichloromethane. The compound crystallizes as solvate **6b**·CH_2Cl_2 in orthorhombic crystal system with the symmetry of the $C222_1$ space group and four units per the unit cell. The structure of **6b** in this crystal structure is depicted in Figure 2.10. Colorless crystals of **6c** for X-ray diffraction analysis experiment were grown similarly. This compound crystallizes in tetragonal crystal system with the symmetry of the $I4_1/a$ space group and four units per the unit cell. The molecular structure of **6c** is shown in Figure 2.11.

Molecular structures of **5a** and **5b** adopt typical heterocubane structures, in which each copper(I) atom has a distorted X_3P tetrahedral coordination environment. All phosphinonitrile ligands coordinate exclusively as P-monodentate donors. The interatomic distances within

the Cu_4X_4 cube in **5a** and **5b** are within the range observed for analogous $[CuX(PPh_3)]_4$ complexes.[68] The faces of the heterocubane moiety are distorted from the ideal square shape. The interface Cu···Cu contacts are always shorter than the X···X distances. This is especially true for **6c**, showing Cu···Cu separations of 2.931(1) Å and I···I distance of 4.344(1) Å. Selected interatomic distances and angles are presented in Tables 2.10 and 2.11. The structure of **6c** was already published in 2016,[59] though without much details.

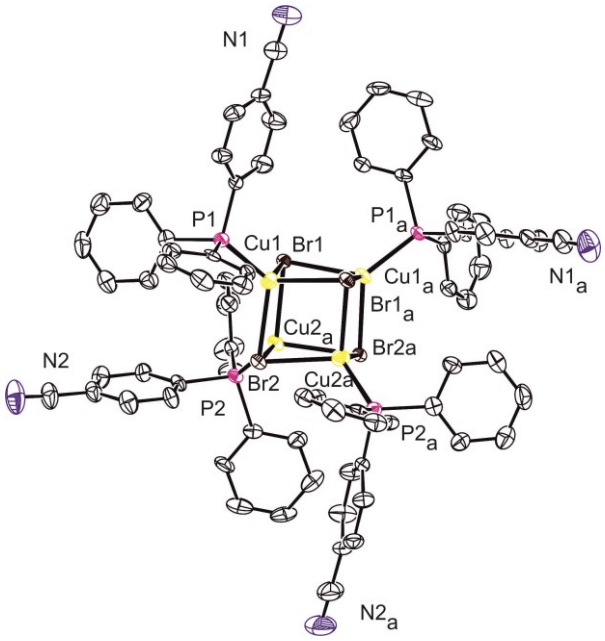

Figure 2.10: Molecular structure of **6b**. Displacement ellipsoids are shown at the 50% probability level. The hydrogen atoms are not shown.

Table 2.10: Selected data for complexes **6c** (in Å and °).

Cu-I	2.639(1)	Cu-Ia-Cua	67.2(1)
Cu-Ib	2.744(1)	Cu-Ia-Cuc	65.6(1)
Cuc-Ia	2.657(1)	Ic-Cua-Ia	110.7(1)
Cua-Cuc	2.917(1)	Cuc-Ia-Cu	67.70(1)
P-Cu	2.259(1)	P-Cu-Ia	109.0(1)
C7-N	1.147(5)	P-Cu-I	116.3(1)
I-Ib	4.344(1)	P-Cu-Ib	103.0(1)
Cu-Cuc	2.931(1)	C4-C7-N	178.1(4)

Table 2.11: Selected data for complexes **6b** (in Å and °).

Br1-Cu1	2.594(1)	Cu1-Cu2	3.302(2)
Br1-Cu2	2.592(1)	Cu1-Cu2a	3.136(1)
Br2-Cu1	2.541(1)	Cu1-Cu1a	3.478(1)
Br2-Cu2	2.536(1)	Br1-Cu1-Br1a	92.5(1)
Cu1-Cu1a	3.478(1)	Cu2-Br1-Cu1	80.4(1)
Cu1-Cu2	3.302(2)	Cu2-Br2-Cu1	81.1(1)
Cu2-Cu2a	3.239(2)	Br1-Cu2-Br2	99.3(1)
Cu1-P1	2.211(2)	Br2a-Cu2-Br1	103.7(1)
Cu2-P2	2.193(2)	N1-C7-C4	176.8(8)
N1-C7	1.128(2)	N2-C27-C24	178.5(2)
N2-C27	1.142(2)		

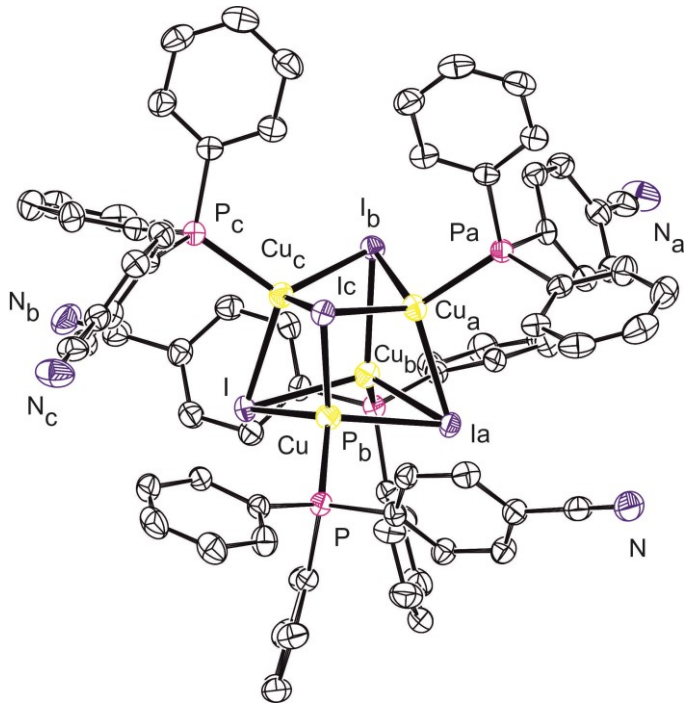

Figure 2.11: Molecular structure of **6c**. Displacement ellipsoids are shown at the 50% probability level. Hydrogen atoms are omitted.

The structure of [{μ(C,N)-MeCN}Cu(L^o-κ*P*)]$_n$ (7)

Colorless crystals of **7** suitable for single-crystal X-ray diffraction analysis resulted by liquid-phase diffusion of hexane into the solution of **7** in dichloromethane. The compound crystallizes in monoclinic crystal system with the symmetry of the $P2_1/c$ space group. The structure of compound **7** is shown in Figure 2.12. For clarity, all hydrogen atoms are omitted.

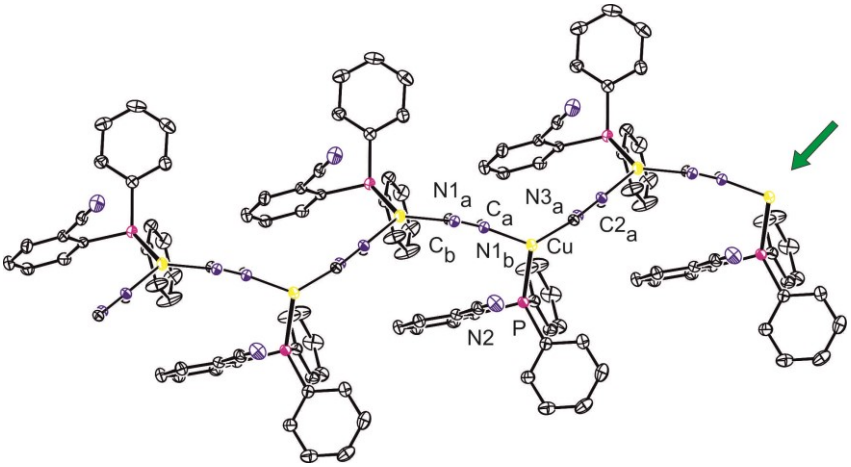

Figure 2.12: Molecular structure of **7**. Displacement ellipsoids are shown at the 50% probability level. The arrows indicate propagation of polymeric chain. For clarity, all hydrogen atoms are omitted.

Table 2.12: Selected data for complex **7** (in Å and ˚).

Cu-P	2.271(1)	P-Cu-C20Ab	123.7(6)
Cu-N20B	2.99(2)	P-Cu-N20Bb	125.1(5)
Cu-N20Bb	2.00(2)	P-Cu-N20A	106.1(6)
Cu-C20A	1.99(2)	Pb-Cub-C20B	105.8(7)
Cu-C20Ab	1.791(2)	N20A-Cu-N20Bb	127.0(8)
Cu-Cua	4.918(1)	C20B-Cu-C20Ab	127.9(10)

Compound **7** is a one-dimensional coordination polymer, in which phosphinonitrile ligands coordinate as P-monodentate donors. Thus resulting identical Cu**L**^{o} units are interlinked into an infinitive ribbon through disordered cyanide bridges that complete trigonal

coordination sphere around the Cu(I) ions. Selected interatomic distances and angles are presented in Table 2.12. Similar type of polymer complex was prepared by the reaction of copper(I) cyanide with tricyclohexylphosphine.[69]

The structure of [{μ(P,N)-L°}$_2${Cu(H$_2$O)(MeCN)}$_2$][BF$_4$]$_2$ (8)

Colorless crystals of **8** used for X-ray diffraction analysis were obtained by liquid-phase diffusion of hexane into a solution of **8** in ethyl acetate. The compound crystallizes in monoclinic crystal system with the symmetry of the $P2_1/c$ space group and two formula units per the unit cell. The structure of **8** is presented in Figure 2.13.

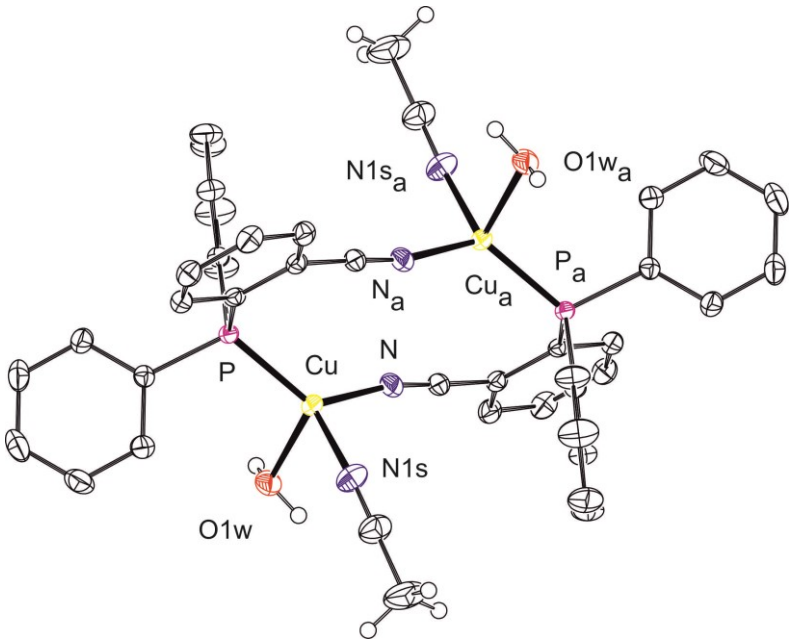

Figure 2.13: Molecular structure of **7**. Displacement ellipsoids are shown at the 50% probability level. The BF_4^- anions are not shown for clarity.

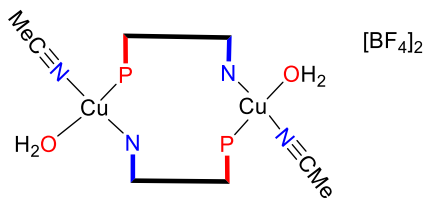

Scheme 2.8: The structure of **8**.

Complex **8** is a dimer, in which two **L°** donors bridge equivalent Cu(MeCN)(H_2O) units. The copper(I) centers are thus coordinated by MeCN, H_2O and two ligands constituting irregular tetrahedrons (Scheme 2.8). Selected interatomic distances and angles are presented in Table 2.13. This kind of structure is rarely seen in literature. A remotely similar structure was reputed for a copper(I) complex with 1-(2-(diphenylphosphino)phenyl)-4-phenyl-1*H*-1,2,3-triazole.[70]

Table 2.13: Selected data for complexes **8** (in Å and °).

Cu-P	2.187(1)	P-Cu-O1w	108.0(1)
Cu-Na	1.988(2)	P-Cu-N1S	124.5(1)
Cu-N1S	1.997(2)	P-Cu-Na	127.1(1)
Cu-O1w	2.191(2)	Cac2-Cac1-N1S	179.3(2)
C1S-N1S	1.127(3)	Cac-N1S-Cu	159.4(2)
Na-C7	1.144(2)	N1S-Cu-Na	101.9(1)
Cu-Cua	4.562(1)	N1S-Cu-Ow	92.9(1)
Na-N	3.327(2)	Na-Cu-Ow	92.9(1)

The structure of $[\{\mu(P,N)\text{-}L^o\}_2Cu]_3[BF_4]_3$ (9)

Colorless crystals of **9** for X-ray diffraction analysis experiment were grown by liquid-phase diffusion of hexane into a solution of **9** in dichloromethane. The compound crystallizes as solvate **9**·CH_2Cl_2 in monoclinic crystal system with the symmetry of the *Cc* space group and four units per the unit cell. The structure **9** is depicted in Figure 2.14.

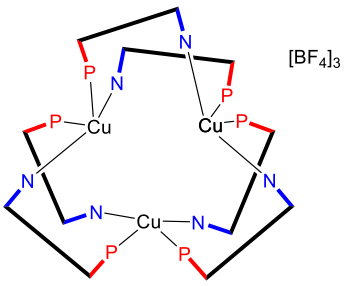

Scheme 2.9: The structure of **9**.

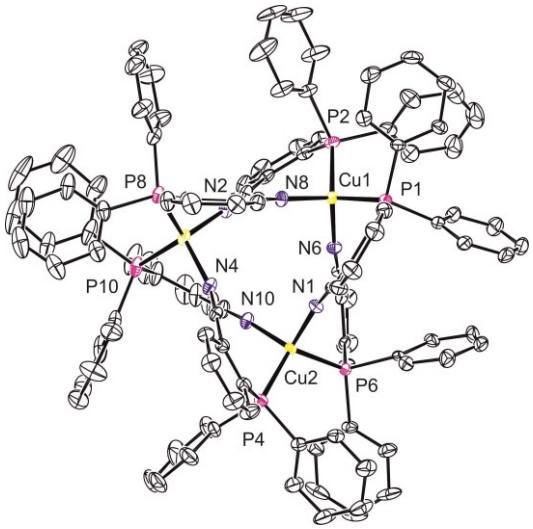

Figure 2.14: Molecular structure of **9**. Displacement ellipsoids are shown at the 50% probability level. The BF_4^- anions and hydrogen atoms are not shown for clarity.

Compound **9** is a cyclic tricopper(I) complex, in which each copper(I) ion is coordinated by four **L^o** ligands (Scheme 2.9). Although each ligand acts as a *P*,*N*-bridge, the structure is asymmetric and every copper(I) atom with distorted N_2P_2 tetrahedral coordination environment is structurally independent (Cu···Cu distances 7.767(1), 4.741(1), 4.833(1) Å). Selected interatomic distances and angles are presented in Table 2.14.

Table 2.14: Selected data for complexes **9** (in Å and °).

	Cu1	Cu2	Cu3
Cu-N	1.992(4)	2.008(4)	1.996(4)
Cu-N‘	2.013(4)	2.017(4)	2.010(4)
Cu-P	2.282(2)	2.260(2)	2.274(2)
Cu-P‘	2.283(2)	2.272(2)	2.275(2)

	Cu1	Cu2	Cu3
N-Cu-N‘	113.7(2)	112.7(2)	114.3(2)
N‘-Cu-P	115.0(2)	106.9(1)	115.5(2)
N-Cu-P‘	99.2(2)	112.2(2)	97.9(2)
N‘-Cu-P‘	101.51(2)	104.0(2)	112.6(2)
N-Cu-P‘	112.6(2)	104.7(2)	99.2(2)

The structure of [{μ(P,N)-L^{o}}$_2$\{Cu(MeOL^{o}-κ*P*)\}$_2$][BF$_4$]$_2$ (10)

Colorless crystals of **10** for X-ray diffraction analysis experiment were obtained by liquid-phase diffusion of hexane into a solution of this complex in chloroform. The compound crystallizes as solvate **10**·6CHCl$_3$ in monoclinic crystal system with the symmetry of the *C*2/*c* space group and four formula units in the unit cell. The structure of compound **10** is shown in Figure 2.15.

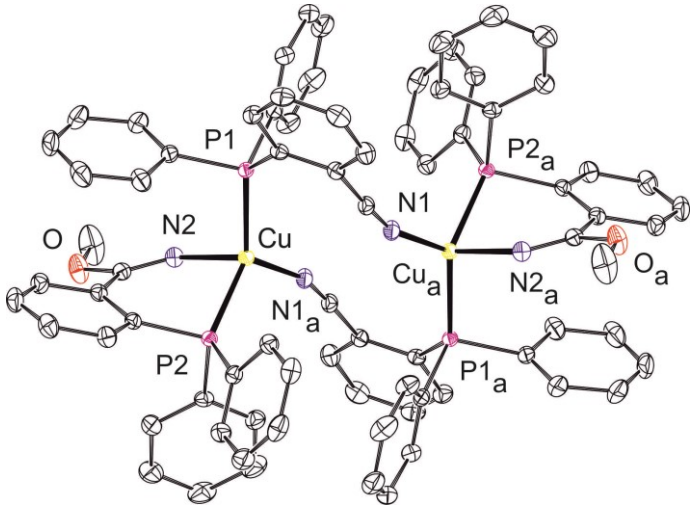

Figure 15: Molecular structure of **10**. Displacement ellipsoids are shown at the 50% probability level. The counter anions and hydrogen atoms are omitted for clarity.

Compound **10** is a dicopper(I) complex built up from two equivalent Cu(MeO-**L^{o}**) units that are connected into dimeric units through asymmetric *P,N*-bridges represented by a pair of **L^{o}** ligands completing distorted tetrahedral coordination spheres around the Cu(I) ions (Scheme 2.10). The Cu-P distances for both types of ligands are the same (Cu-P1 and Cu-P2 = 2.240(1) Å). The Cu-N distance for the nitrogen of the imidate group is slightly longer than for the nitrogen in the nitrile group (2.092(2) Å vs. 2.006(2) Å). Selected interatomic distances and angles are presented in Table 2.14. Compound **10** is the first published copper(I) complex containing coordinated phosphine and imidate groups.

Table 2.15: Selected data for complexes **10** (in Å and °).

Cu-Cua	4.706(1)	N1a-Cu-N2	95.8(1)
Cu-P1	2.240(1)	N1a-Cu-P1	121.4(1)
Cu-P2	2.240(1)	N1a-Cu-P2	109.4(1)
Cu-N1a	2.006(2)	P1-Cu-P2	125.7(1)
Cu-N2	2.092(2)	N2-Cu-P2	86.9 (1)
N1-N1a	3.382(3)	N2-Cu-P1	104.8(1)
N1a-C7a	1.143(3)	Cu-N1a-C7a	162.4(2)
C40-O2	1.435(3)	C40-O2-C27	118.1(2)

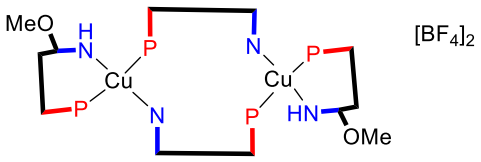

Scheme 2.10: Schematic representation of the structure of **10**.

2.4 Infrared spectra

In the present case, infrared spectroscopy is particularly suitable for following the stretching vibrations of the nitrile groups, which are clearly identified and do not overlap with other bands (Table 2.16). The *ν*(C≡N) bands in all complexes are usually slightly shifted to higher energies (average shift is only about 7 cm^{-1}) compared to the respective uncoordinated ligands (in the case of **6c**, the nitrile band is found at exactly the same position). The shift was observed even when the nitrile group is not involved in coordination. Although many complexes contain two or more non-equivalent ligands coordinating in completely different modes, only one nitrile band is typically observed. Two „nitrile bands" were observed only in the case of complex **7** (due to cyanide group) and **8** (contains acetonitrile). The spectrum of complex **10** possessing a phosphinoimide donor, shows a band attributable to NH stretching vibration at 2238 cm^{-1}.

Table 2.16: Positions of the *ν*(C≡N) bands in the IR spectra.

Complex	**L^o**	**1**	**2**	**3**	**4a**	**4b**	**4c**	**7**
ν [cm^{-1}]	2220	2235	2229	2226	2222	2223	2225	2128[a], 2227

Complex	**8**	**9**	**10**	**L^p**	**5a**	**5b**	**6c**
ν [cm^{-1}]	2278, 2308[b]	2236	2238	2223	2234	2230	2223

[a]*ν*(C≡N) band of CN.[71] [b]*ν*(C≡N) band of MeCN.[72]

2.5 NMR spectra

The synthesized donors **L^o** and **L^p** were characterized by ^{1}H, ^{13}C and ^{31}P NMR spectra which confirmed their purity.[61]

NMR analysis of the complexes in solution furnished only limited information regarding their structures. For instance, the ^{1}H NMR spectra showed only signals of the phenyl groups and were not differentiated. ^{31}P{^{1}H} NMR spectroscopy suggested fluxional nature of the prepared complexes. All measured ^{31}P{^{1}H} NMR signals were broad and, for complexes **3**, **4a**, **5a** and **10**, the ^{31}P{^{1}H} NMR signals were not even detected because of extreme broadening. In some cases (complex **9**), the observation of two signals suggested the presence of several compounds in a solution. Notably, in all complexes with **L^o** the ^{31}P NMR signals shifted downfield confirming coordination of the phosphorus atom. On the other hand, signals of complexes with **L^p** were surprisingly shifted upfield as compared with the free ligand.

2.6 Mass spectra

The most stable ion, which was detected by low-resolution electrospray ionization technique (ESI) for all prepared complexes (with a single exception), was fragment $[Cu(\mathbf{L})_2]^+$ (**L** = **L^o** or **L^p**). Actually, in many cases this was the one and only ion observed in the ESI

mass spectra, which consequently provided only a little insight into the complex stoichiometry or their structure.

The exception was the mass spectrum of cyanide complex **7** showing a fragment ion $[Cu_2CN(\mathbf{L^o})_2]^+$, which probably represents the repeating of this coordination polymer (Scheme 2.11).

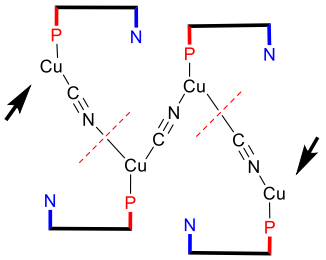

Scheme 2.11: Possible formation of the $[Cu_2CN(\mathbf{L^o})_2]^+$ fragment form **7**.

Fragments of similar type were observed also for the polymeric complexes **5a** and **5b** ($[Cu_2X(\mathbf{L^p})_2]^+$) and for the molecular complexes **1** and **4a** ($[Cu_2X(\mathbf{L^o})_2]^+$). For these polymeric complexes, there are two probable ways of fragmentation based on the original structure (Scheme 2.12). It can be supposed that fragmentation (a) is more likely because of requires breakage of only weaker Cu-N bonds.

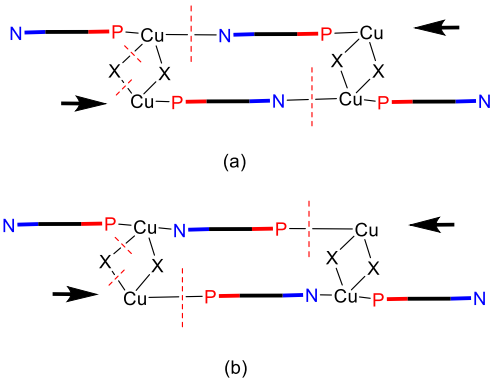

Scheme 2.12: Two possibilities of forming ion $[Cu_2X(\mathbf{L^p})_2]^+$ from the polymeric structure.

Quite a number of fragments was observed in the ESI spectrum of complex **10** which contained phosphinonitrile and phosphinoimidate donor. In additon to the expected fragments $[Cu(MeO\text{-}\mathbf{L^o})(\mathbf{L^o})]^+$ and $[Cu(MeO\text{-}\mathbf{L^o})]^+$, there were also observed fragments $[Cu(\mathbf{L^o})_2]^+$ and $[Cu(MeO\text{-}\mathbf{L^o})_2]$ presumably resulting by random redistribution in solution or during the ionization.

In the spectra of **3** and **5b** were also observed adducts with alkali metal ions, namely $[Cu(\mathbf{L^p})_2BrK]^+$ and $[CuI(\mathbf{L^o})Na]^+$.

2.7 Catalysis

Since the prepared complexes exhibit diverse structures, and are accessible from simple and easily synthesized ligands, we have decided to test them as defined catalysts. The majority of the prepared complexes are polynuclear in nature. In 2013, dinuclear copper intermediate was postulated in catalytic cycle pathway of copper-catalyzed alkyne-azide cycloaddition reaction (CuAAC) which made us to choose this reaction for catalytic testing. (Scheme 2.13).[73]

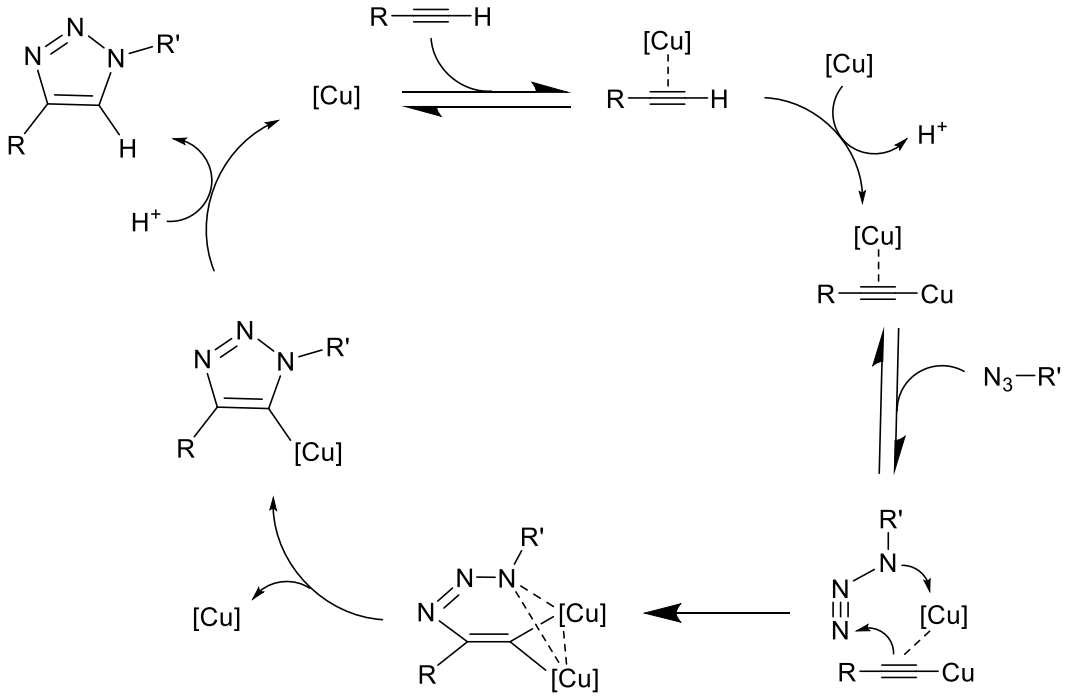

Scheme 2.13: Plausible mechanism of copper-catalyzed alkyne-azide cycloaddition.[73]

For screening experiments, we used the coupling of commercially available benzyl azide (available as 0.5 M solution in dichloromethane) and phenylacetylene in presence of 0.5 mol.% of catalyst (Scheme 2.14). The reaction was monitored after 2 h. The obtained results are collected in Table 2.17.

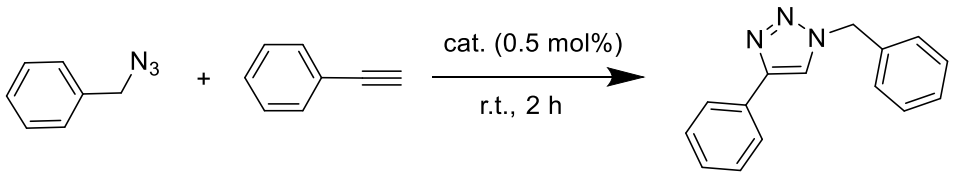

Scheme 2.14: Reaction used for the initial screening experiments.

Table 2.17: Catalytic results achieved with various phosphinonitrile complexes and CuCl.

Compound Number	Structure	NMR yield [%][a]
1	$[Cu_4Cl_4(\mathbf{L^o})_3]$	24
4a	$[CuCl(\mathbf{L^o})_2]$	13
2	$[CuBr(\mathbf{L^o})]_4$	17
4b	$[CuBr(\mathbf{L^o})_2]$	14
3	$[CuI(\mathbf{L^o})_2 \cdot CuI \cdot CuI(\mathbf{L^o}) \cdot 2CHCl_3]_n$	5
4c	$[CuI(\mathbf{L^o})_2]$	21
7	$[CuCN(\mathbf{L^o})]_n$	17
5a	$[CuCl(\mathbf{L^p})]_n$	18
5b	$[CuBr(L^p)]_n$	9
6c	$[CuI(L^p)]_4$	6
	CuCl	10

[a] The results are average of two experiments.

The most satisfactory yelds of 1,2,3-triazole (24%) were obtained with catalyst **1**. However, even such a result is relatively poor upon comparing the catalytic efficacy of CuCl itself (10%) and, mainly, the results reported in the literature (0.1% cat, 10 min, ≈ 100% yield).[17] This lead us to abandon further reaction tests.

2.8 Luminescence studies

Copper(I) compounds are attracting considerable attention as promising luminescent materials. This led us to investigate optical properties of complexes reported in this Thesis.

The diffuse reflectance spectra were recorded for all defined halide complexes (compounds **1**-**6**), whose purity was confirmed by elemental analysis. The spectra were analyzed by the Kubelka-Munk function, providing a correlation between the reflectance and concentration. The concentrations of an absorbing species were determined using the Kubelka-Munk formula:[74]

$$F(R) = (1 - R)^2/2R = k/s = Ac/s$$

where R = reflectance, k = absorption coefficient, s = scattering coefficient, c = concentration of the absorbing species, and A = absorbance.

The absorption spectra measured in the solid state are shown in Figures 2.16 and 2.17. The spectra exhibit broad bands around 260 nm, which is characteristic of an arylphosphine. This band can be tentatively assigned to a mixed $n \rightarrow \pi^*$ and $\pi \rightarrow \pi^*$ transition; the former being the transition of an electron from the lone pair orbital on phosphorus to an empty antibonding orbital on the phenyl ring.[75] A stung band at 350-410 nm can be attributed to an electronic transition involving by the copper, the halide ligands, or both.[76] Positions of these maxima consequently correspond to the type of structure: compounds **4a-c** (360, 358, 347 nm), compounds **5b-c** (383, 384 nm).

All studied complexes are emissive (λ_{exc} = 390 nm) in the solid state at room temperature with emission maxima in the range from 522 to 573 nm (Figure 2.18 and 2.19, Table 2.17). For polynuclear complexes, a common feature is the mixing of electron states so that an assignment of electron state with concepts drawn from simple one-electron transitions may be quite misleading.[30] The shifts of emission maxima are independent on the type of halide atoms: 526, 562, 573 nm for chloride, 522, 523, 560 nm for bromide, 506, 523, 559 nm for iodide. The shifts of the emission maxima for mononuclear complexes **4a-c** do not follow the trend in ligand field splitting ($I^- < Br^- < Cl^-$).[77] However, the shifts appear to be characteristic of the particular structure (for example „open squares" structures **2** and **3** emit

at 522 and 523 nm, while the polymeric structures **5a** and **5b** show emission maxima at 562 and 560 nm).

Table 2.17: Absorption and emission maxima of halide complexes (λ_{exc} = 390 nm).[a]

Compound	**1**	**2**	**3**	**4a**	**4b**	**4c**	**5a**	**5b**	**6c**
λ_{abs}	387	405	408	360	358	347	383	384	410
λ_{em}	526	522	523	573	523	559	562	560	506

[a] all maxima in nm.

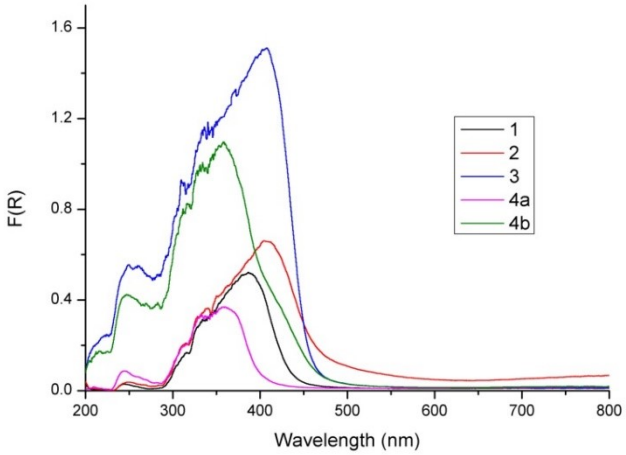

Figure 2.16: Uv-vis absorption spectra of compounds **1-4b** as crystals at 298 K.

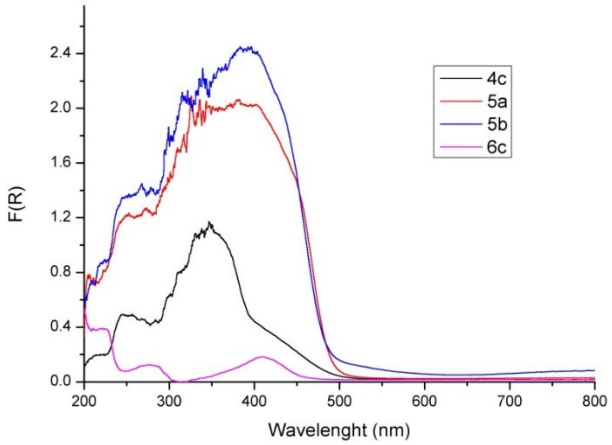

Figure 2.17: Uv-vis absorption spectra of compounds **4c-6c** as crystals at 298 K.

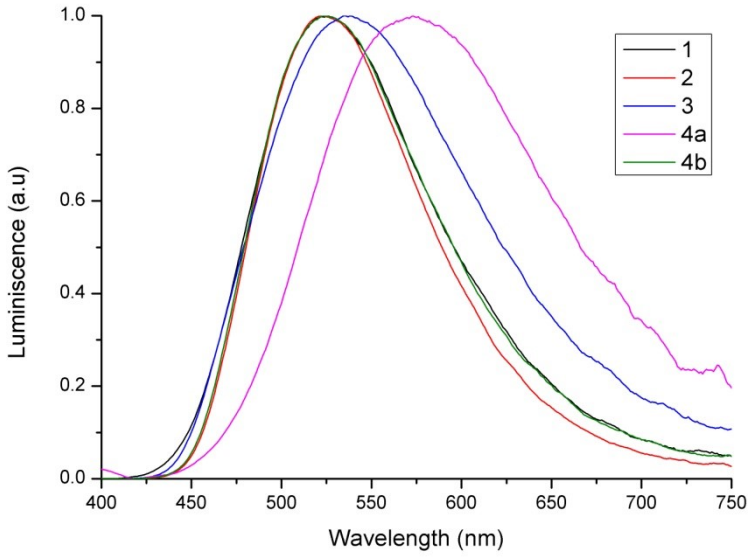

Figure 2.18: Normalized emission spectra of compounds **1-4b** as crystals at 298 K (λ_{exc} = 390 nm).

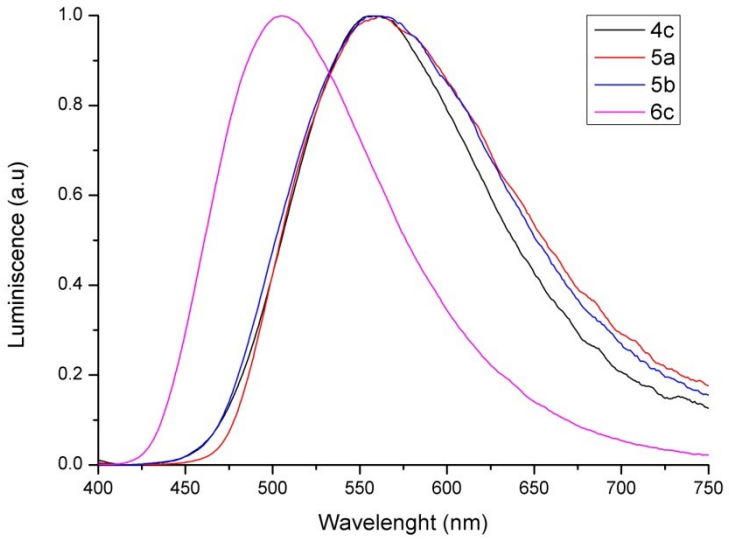

Figure 2.19: Normalized emission spectra of compounds **4c-6c** as crystals at 298 K (λ_{exc} = 390 nm).

3. Summary

The main aim of this Thesis was the investigation of coordination properties of a pair of isomeric phosphinonitrile donors that are poorly described in the literature. A series of new copper(I) complexes with these donors were successfully synthesized and fully characterized by nuclear magnetic resonance, infrared spectroscopy and elemental analysis, mass spectrometry, and their solid-state structures were determined by single-crystal X-ray crystallography.

X-ray crystallographic analysis revealed mononuclear, polynuclear or even polymeric structure with unusual distorted trigonal or tetrahedral coordination environments around the copper(I) ions. In these complexes, the phosphinonitrile ligands act as *P*-monodentate or *P*,*N*-bridging donors. All Cu halide complexes investigated in this work are luminescent. Emission and absorption spectra were received in the solid state. Besides, newly prepared compounds were tested as catalysts in copper-catalyzed alkyne-azide cycloaddition. Unfortunately, they showed only poor catalytic activity for this particular reaction system.

4. Experimental

4.1 Material and methods

All reactions were performed under an argon atmosphere using standart Schlenk techniques.[78] Anhydrous dichloromethane and methanol were obtained from a PureSolv MD5 Solvent Purification System (Innovate Technology Inc., USA). Other chemicals (Alfa-Aesar or Sigma Aldrich) and solvents (reagent grade from Lach-Ner, Czech Republic) were used without any additional purification.

NMR spectra were recorded at 298 K on a Varian Unity Inova 400 spectrometer (^{1}H, 399.95 MHz; ^{13}C, 100.58 MHz; and ^{31}P, 161.90 MHz). Chemical shifts (δ/ppm) are given relative to internal tetramethylsilane (^{1}H and ^{13}C NMR) and to external 85% aqueous H_3PO_4 (^{31}P), respectively.

Conventional low-resolution electrospray ionization mass spectra (ESI MS) were recorded with an Esquire 3000 spectrometer (Bruker). The samples were dissolved in HPLC-grade methanol.

Infrared spectra were collected on Nujol mulls using an FTIR Thermo Fisher Nicolet 760 instrument. The range investigated was 400-4000 cm^{-1}.

The UV/Vis absorption spectra were recorded on a Varian 4000 spectrometer equipped with an integration sphere. The powder samples were placed at the entrance of the sphere and measured in the diffuse reflectance mode to minimize light scattering. The Kubelka-Munk function was used for the analysis of these diffuse reflectance spectra. The steady-state fluorescence spectra were monitored using an FLS 980 (Edinburgh Instruments, UK) spectrofluorimeter using a holder for powdery samples.

Diffraction data were collected at 150(2) K with a Nonius Kappa CCD diffractometer equipped with an Apex II image plate detector and Cryostream Cooler (Oxford Cryosystem) using graphite-monochromated Mo Kα radiation (λ = 0.71073 Å). The data were processed and corrected for absorption by the methods included in the diffractometer software. The

structures were solved by direct methods (SHELX97[79]) and refined by full-matrix least-squares routines based on F^2 (SHELXL97[79]). All geometric calculations were carried out, and the structural diagrams were obtained with a recent version of the PLATON program.[80]

4.2 Catalysis

General procedure for copper catalyzed alkyne-azide cycloaddition of benzyl azide and phenylacetylene to give 1-benzyl-4-phenyl-1,2,3-triazole

The respective Cu(I) complex (0.5 mol.% with respect to a simple [Cu] unit), benzyl azide (1.00 mmol, 2 ml of 0.5 M in CH_2Cl_2) and phenylacetylene (1.00 mmol, 0.11 ml) were added to a Schlenk tube, The reaction vessel was filled with argon and sealed with a rubber septum. The mixture was stirred for 2 h at room temperature and then evaporated under vacuum. The yield was determined by integration of ^{1}H NMR spectrum.

4.3 Syntheses

Synthesis of 2-(diphenylphosphino)benzonitrile (L^o)[58]

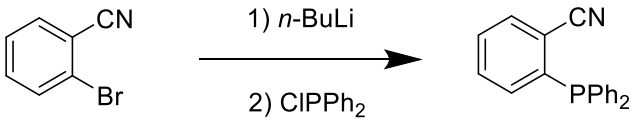

To a solution of 2-bromobenzonitrile (10.93 g, 60.0 mmol) in Et_2O (300 ml) and THF (60 ml) under argon was added 1.6 M *n*-BuLi in hexane (37.6 ml, 60.2 mmol) at −78 °C. After stirring for 10 min, a solution of (choro)diphenylphosphine (10.7 ml, 60.0 mmol) in THF (60 ml) was slowly introduced within 45 min. The resulting mixture was stirred at −78 °C for additional 3 h, then allowed to warm up to room temperature, and stirred overnight. The red-brown suspension was treated with saturated $NaHCO_3$ (90 ml) and stirred for another 10 min. The aqueous layer was separated and extracted with Et_2O (200 ml). The combined organic layers were dried over $MgSO_4$ and evaporated, leaving crude product which was purified by column chromatography (silica gel, Et_2O/hexane, 1:3). Finally, the product was dissolved in hot *i*-PrOH (ca 20 ml) and the solution cooled to room temperature. The separated colorless

crystals were collected on a frit and dried under vacuum. Yield of **L^{o}**: 5.54 g (32 %), colorless crystals.

Characterization: ^{1}H NMR ($CDCl_3$): δ 7.02-7.06 (m, 1 H), 7.27-7.50 (m, 12 H), 7.85 (m, 1 H). $^{13}C\{^{1}H\}$ NMR ($CDCl_3$): δ 117.59 (d, $^{1}J_{CP}$ = 4 Hz, 1 C, 6b), 117.91 (d, $^{3}J_{CP}$ = 33.0 Hz, 1C, 7b), 128.76 (s, 2 C, 4p), 128.81 (s, 1 C, 3b), 129.40 (s, CH, 4 C, 3p), 132.37 (s, CH, 1 H, 4b), 133.39 (s, 1 C, 5b), 133.71 (d, $^{2}J_{CP}$ = 5 Hz, 1 C, 2b), 134.01 (d, $^{2}J_{CP}$ = 20 Hz, 4 C, 2p), 134.63 (d, $^{1}J_{CP}$ = 10 Hz, 2 C, 1p), 143.02 (d,$^{1}J_{CP}$ = 20 Hz, 1 C, 1b). $^{31}P\{^{1}H\}$ NMR ($CDCl_3$): δ −7.9 (s). IR (Nujol, cm^{-1}): 2220 m, 1582 w, 1434 s, 1307 w, 1281 w, 1188 w, 1154 w, 1127 w, 1091 w, 1070 w, 1024 w, 997 w, 918 w, 851 w, 764 s, 750 s, 742 s, 727 m, 705 m, 694 m, 579 w, 560 w, 521 w, 504 m, 488 m, 429 w.

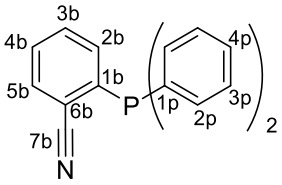

$^{13}C\{^{1}H\}$ NMR signals were assigned according to the literature.[61]

Synthesis of 4-(diphenylphosphino)benzonitrile (L^{p})[60]

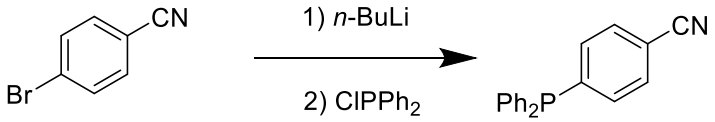

To a solution of 4-bromobenzonitrile (5.10 g, 28.0 mmol) in THF (85 mL) and hexane (20 mL) was added 1.6 M *n*-BuLi in hexane (11.2 ml, 28.0 mmol) at −78 °C. After stirring for 5 min, neat (chloro)diphenylphosphine (5.2 mL, 29.0 mmol) was added and the mixture was stirred at −78 °C for 1 hour and then at room temperature for additional 2 h. The product was extracted with THF (3 x 60 ml), washed with 1 M NaOH (60 ml), saturated NaCl (60 ml) and the combined organic layers were dried over $MgSO_4$. The crude product obtained by evaporating was purified by column chromatography (silica gel, AcOEt/ Hx, 1:5), the solvent was evaporated and the solid dissolved in hot heptane. Charcoal was added and the mixture was filtered and evaporated. Yield of **L^{p}**: 3.22 g (40%), white solid. Crystal for X-ray diffraction analysis was obtained by slow cooling of a heptane solution down to −20 °C.

Characterization: ^{1}H NMR ($CDCl_3$): δ 7.28-7.41 (m, 12 H), 7.55-7.59 (m, 2 H). $^{13}C\{^{1}H\}$ NMR ($CDCl_3$): δ 111.89 (s, 1 C, 4b), 118.71 (s, 1 C, 5b), 128.84 (d, $^{3}J_{CP}$ = 7 Hz, 4 C, 3p), 129.47 (s, 2 C, 4p), 131.68 (d, $^{3}J_{CP}$ = 6 Hz, 2 C, 3b), 133.47 (d, $^{2}J_{CP}$ = 19 Hz, 2 C, 2b), 134.01 (d, $^{2}J_{CP}$ = 20 Hz, 4 C, 2p), 135.35 (d, $^{1}J_{CP}$ = 10 Hz, 2 C, 1p), 145.10 (d, $^{1}J_{CP}$ = 17 Hz, 1 H, 1b). $^{31}P\{^{1}H\}$ NMR ($CDCl_3$): δ −3.7 (s). IR (Nujol, cm^{-1}): 2223 m, 1659 w, 1593 m, 1570 w, 1546 w, 1488 m, 1396 w, 1311 m, 1273 m, 1202 w, 1180 w, 1157 w, 1087 w, 1020 w, 1026 w, 999 w, 977 w, 955 w, 923 w, 859 w, 825 m, 757 m, 747 m, 666 w, 576 w, 549 m, 502 m, 490 m, 471 m, 412 w.

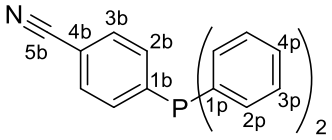

$^{13}C\{^{1}H\}$ NMR signals were assigned according to the literature.[61]

Synthesis of [(μ-Cl)$_3$(μ$_3$-Cl)Cu$_4$(L^o-κ*P*){μ(P,N)-L^o}$_2$] (1)

$$CuCl + \mathbf{L^o} \longrightarrow [Cu_4Cl_4(\mathbf{L^o})_3]$$

Solution of **L^o** (57.5 mg, 0.20 mmol) in dichloromethane (8 mL) was added to a suspension of copper(I) chloride (19.8 mg, 0.20 mmol) in the same solvent (2 mL). The resulting colorless mixture was stirred for 1.5 h. Following evaporation, the solid residue was dissolved in a small amount of ethyl acetate and dichloromethane (1:1). The solution was filtered (PTFE syringe filter, 45 μm pore size) and layered with hexane. Crystallization by liquid-phase diffusion over several days gave colorless crystals of **1**. Yield: 46 mg (73 %).

Characterization: ^{1}H NMR ($CDCl_3$): δ 7.16-7.22 (m, 1 H), 7.32-7.58 (m, 12 H), 7.62-7.67 (m, 1 H). $^{31}P\{^{1}H\}$ NMR ($CDCl_3$): δ −3.7 (br s). IR (Nujol, cm^{-1}): 3052 m, 2725 w, 2235 m, 1583 w, 1313 m, 1287 w, 1263 m, 1196 w, 1168 w, 1160 w, 1129 w, 1095 s, 1067 w, 1027 m, 998 m, 885 w, 846 w, 759 s, 748 s, 735 s, 697 s, 672 w, 582 m, 556 w, 533 m, 502 s, 482 m, 438 w. ESI+ MS: *m/z* 450.0 ([Cu_2(**L^o**)Cl]). 637.1 ([Cu(**L^o**)$_2$]$^+$). Anal. Calcd for $C_{57}H_{42}N_3Cl_4Cu_4P_3$ (1257.8): C 54.42, H 3.37, N 3.34 %. Found: C 53.99, H 3.56, N 3.24 %.

Synthesis of $[(\mu\text{-Br})_2(\mu_3\text{-Br})_2Cu_4(L^o\text{-}\kappa P)_2\{\mu(P,N)\text{-}L^o\}_2]$ (2)

$$CuBr{\cdot}SMe_2 + \mathbf{L^o} \longrightarrow [Cu_4Br_4(\mathbf{L^o})_4]$$

Solution of $\mathbf{L^o}$ (57.5 mg, 0.2 mmol) in dichloromethane (6 mL) was added to a suspension of copper(I) bromide-dimethyl sulfide complex (41.1 mg, 0.2 mmol) in the same solvent (4 mL). The resulting yellow mixture was stirred for 1.5 h. After evaporation under vacuum, the solid crude product was dissolved in a small amount of 1,2-dichloroethane, the solution was filtered (PTFE syringe filter, 45 µm pore size) and layered with hexane. Crystallization by liquid-phase diffusion over several days provided yellow crystals of **2**. Yield: 74 mg (86%).

Characterization: ^{1}H NMR ($CDCl_3$): δ 7.20-7.26 (m, 1 H), 7.32-7.39 (m, 4 H), 7.41-7.52 (m, 4 H), 7.54-7.61 (m, 4 H), 7.67-7.72 (m, 1 H). $^{31}P\{^1H\}$ NMR ($CDCl_3$): δ −4.8 (br s). IR (Nujol, cm^{-1}): 2229 w, 1668 w, 1561 w, 1309 w, 1182 w, 1098 m, 1027 w, 1018 w, 999 w, 829 m, 749 m, 695 s, 660 w, 619 w, 597 w, 552.6 m, 512 m, 495 w, 484 w, 412 w. ESI+ MS: *m/z* 637.1 ($[Cu(\mathbf{L^o})_2]^+$). Anal. Calcd for $C_{76}H_{56}N_4Br_4Cu_4P_4$ (1722.9): C 52.98, H 3.28, N 3.25%. Found: C 52.86, H 3.31, N 3.21%.

Synthesis of $[(\mu_3\text{-I})Cu(\mu\text{-I})_2Cu_2\{\mu(P,N)\text{-}L^o\}_2]_n$ (3)

$$CuI + \mathbf{L^o} \longrightarrow [CuI(\mathbf{L^o}){\cdot}CuI{\cdot}CuI(\mathbf{L^o})]_n$$

Solution of $\mathbf{L^o}$ (57.5 mg, 0.20 mmol) in dichloromethane (7 mL) was added to a suspension of copper(I) iodide (38.09 mg, 0.2 mmol) in the same solvent (3 mL). The resulting yellow mixture was stirred for 2 h. The solid residue obtained after evaporation was dissolved in a small amount of chloroform, the solution was filtered (PTFE syringe filter, 45 µm pore size) and layered with hexane. Crystallization by liquid-phase diffusion gave yellow-white crystals of **3**·2$CHCl_3$. Crystals were isolated by suction and dried under vacuum. Yield of **3**·$CHCl_3$: 59 mg (54%).

Characterization: ^{1}H NMR ($CDCl_3$): δ 7.32-7.36 (m, 5 H, PPh_2), 7.41-7.46 (m, 5 H, PPh_2), 7.48-7.52 (m, 4 H, C_6H_4). IR (Nujol, cm^{-1}): 3056 w, 2226 m, 1582 w, 1307 w, 1192 w, 1165

w, 1096 m, 1027 w, 996 w, 767 m, 756 s, 744 m, 725 w, 693 m, 578 w, 526 m, 501 s, 480 w, 435 w. ESI+ MS: *m/z* 499.9 ([Cu(**L**^{o})INa]$^{+}$), 637.1 ([Cu(**L**^{o})$_2$]$^{+}$). Anal. Calcd for $C_{38}H_{28}N_2Cu_3I_3P_2 \cdot CHCl_3$ (1265.3): C 37.02, H 2.31, N 2.21%. Found: C 36.93, H 2.36, N 2.18%.

Synthesis of [CuCl(L^{o}-κ*P*)$_2$] (4a)

$$CuCl + 2\ \mathbf{L}^{o} \longrightarrow [CuCl(\mathbf{L}^{o})_2]$$

Solution of **L^{o}** (40.2 mg, 0.14 mmol) in dichloromethane (5 mL) was added to a suspension of copper(I) chloride (6.9 mg, 0.07 mmol) in the same solvent (2 mL). The resulting colorless mixture was stirred for 1.5 h. and evaporated under vacuum. The solid residue was dissolved in a small amount of ethyl acetate, the solution was filtered (PTFE syringe filter, 45 μm pore size) and layered with hexane. Crystallization by liquid-phase diffusion over several days furnished colorless crystals of **4a**. Yield: 35 mg (74 %).

Characterization: ^{1}H NMR ($CDCl_3$): δ 7.29-7.36 (m, 5 H), 7.39-7.44 (m, 3 H), 7.47-7.58 (m, 6 H). ^{31}P{^{1}H} NMR ($CDCl_3$): δ −3.6 (br s). IR (Nujol, cm^{-1}): 3054 m, 2679 w, 2222 m, 1964 w, 1736 w, 1661 w, 1586 w, 1572 w, 1315 w, 1281 w, 1191 w, 1157 w, 1124 m, 1098 s, 1028 w, 997 m, 965 w, 889 w, 850 w, 773 s, 751 s, 697 s, 618 w, 578 w, 525 s, 505 s, 496 m, 474 w, 442 w, 424 w, 408 w. ESI+ MS: *m/z* 637.1 ([Cu(**L**^{o})$_2$]$^{+}$), 737.0 ([Cu$_2$(**L**^{o})$_2$Cl]). Anal. Calcd for $C_{38}H_{28}N_2ClCuP_2$ (673.6): C 67.76, H 4.19, N 4.16 %. Found: C 67.33, H 4.36, N 3.89 %.

Synthesis of [CuBr(L^{o}-κ*P*)$_2$] (4b)

$$CuBr \cdot SMe_2 + 2\ \mathbf{L}^{o} \longrightarrow [CuBr(\mathbf{L}^{o})_2] + [Cu_4Br_4(\mathbf{L}^{o})_4]$$

Solution of **L^{o}** (40.2 mg, 0.14 mmol) in dichloromethane (8 mL) was added to a suspension of copper(I) bromide-dimethyl sulfide complex (14.4 mg, 0.07 mmol) in the same solvent (4 mL) and the colorless reaction mixture was stirred for 2 h. After evaporation, the crude product was dissolved in a small amount of ethyl acetate, the solution was filtered (PTFE syringe filter, 45 μm pore size) and layered with hexane. Crystallization by liquid-phase diffusion over several days afforded white crystals of **4b** and yellow of **2**. The crystals were

isolated by suction, dried under vacuum and separated under a microscope. Yield of **4b**·1/50AcOEt: 38 mg (75%). Yield of **2**·1/50AcOEt: 4 mg (13%).

Characterization data for **2**·1/50AcOEt: Anal. Calcd $C_{19}H_{14}NBrCuP$·1/50AcOEt (436.2): C 63.15, H 3.98, N 3.87%. Found: C 62.85, H 3.84, N 3.53%.

Characterization data for **4b**·1/50AcOEt: ^{1}H NMR ($CDCl_3$): δ 7.25-7.34 (m, 5 H), 7.39-7.44 (m, 5 H), 7.48-7.58 (m, 4 H). $^{31}P\{^{1}H\}$ NMR ($CDCl_3$): δ −3.7 (br s). IR (Nujol, cm^{-1}): 3051 w, 2223 m, 1572 w, 1583 w, 13115 m, 1280 m, 1266 w, 1097 s, 1072 w, 1026 m, 997 m, 969 w, 931 w, 885 w, 845 w, 763 s, 756 m, 744 m, 726 m, 670 m, 672 w, 619 w, 578 m, 527 s, 503 s, 474 m, 433 w, 410 m. ESI+ MS: *m/z* 637.1 ($[Cu(\mathbf{L^o})]^+$). Anal. Calcd for compound **4b**: $C_{38}H_{28}CuN_2P_2Br$·1/50AcOEt (723.4): C 52.43, H 3.26, N 3.21%. Found: C 52.41, H 3.28, N 2.39%.

Synthesis of [CuI(L^o-κ*P*)$_2$] (4c)

$$CuI + 2\ \mathbf{L^o} \longrightarrow [CuI(\mathbf{L^o})_2]$$

Solution of $\mathbf{L^o}$ (46.0 mg, 0.16 mmol) in dichloromethane (6 mL) was added into a suspension of copper(I) iodide (15.2 mg, 0.08 mmol) in the same solvent (2 mL) and the obtained colorless mixture was stirred for 2 h and then evaporated. The solid residue was dissolved in a small amount of chloroform, the solution was filtered (PTFE syringe filter, 45 μm pore size) and layered with hexane. Crystallization by liquid-phase diffusion over several days afforded colorless crystals of **4c**. Yield: 51 mg (83%).

Characterization: ^{1}H NMR ($CDCl_3$): δ 7.31-7.36 (m, 5 H), 7.40-7.46 (m, 5 H), 7.48-7.61 (m, 4 H). $^{31}P\{^{1}H\}$ NMR ($CDCl_3$): δ −4.9 (br s). IR (Nujol, cm^{-1}): 3056 w, 2676 w, 2225 m, 1835 w, 1581 w, 1306 w, 1279 w, 1266 w, 1164 w, 1095 m, 1072 w, 1026 w, 1004 w, 995 w, 882 w, 766 m, 756 s, 725 m, 707 m, 699 s, 690 m, 673 w, 619 w, 579 w, 555 w, 526 s, 501 s, 481 m, 434 w, 411 w. ESI+ MS: *m/z* 637.0 ($[Cu(\mathbf{L^o})_2]^+$). Anal. Calcd for $C_{38}H_{28}N_2CuIP_2$ (765.0): C 59.66, H 3.69, N 3.66%. Found: C 59.21, H 3.60, N 3.31%.

Synthesis of [{μ(P,N)-L^{p}}Cu(μ-Cl)]$_n$ (5a)

$$CuCl + \mathbf{L^{p}} \longrightarrow [CuCl(\mathbf{L^{p}})]_n$$

Solution of **L^{p}** (57.5 mg, 0.20 mmol) in dichloromethane (8 mL) was added to a suspension of copper(I) chloride (19.8 mg, 0.20 mmol) in the same solvent (2 mL). The resulting colorless mixture was stirred for 1.5 h and evaporated, leaning a solid residue, which was immediately dissolved in a small amount of chloroform. The solution was filtered (PTFE syringe filter, 45 μm pore size) and layered with hexane. Crystallization by liquid-phase diffusion furnished yellow crystals of **5a**·2$CHCl_3$. The crystals were isolated by suction and dried under vacuum. Yield of **5a**·1/20$CHCl_3$: 50 mg (56%).

Characterization: ^{1}H NMR ($CDCl_3$): δ 7.27-7.33 (m, 4 H), 7.39-7.57 (m, 10 H). IR (Nujol, cm^{-1}): 3045 m, 2726 w, 2234 m, 1671 w, 1593 s, 1310 m, 1007 w, 1182 m, 1158 w, 1096 s, 1070 w, 1027 m, 1019 m, 998 w, 969 w, 920 w, 831 s, 756 s, 744 s, 718 m, 696 s, 619 w, 592 m, 554 s, 511 s, 495 m, 432 w, 410 w. ESI+ MS: *m/z* 637.1 ([Cu(**L^{p}**)$_2$]$^+$), 737.0 ([Cu_2(**L^{p}**)$_2$Cl]$^+$). Anal. Calcd for $C_{19}H_{14}NClCuP$·1/20CH_2Cl_2 (390.5): C 58.33, H 3.61, N 3.57%. Found: C 58.21, H 3.54, N 3.33%.

Synthesis of [{μ(P,N)-L^{o}}Cu(μ-Br)]$_n$ and [(μ$_3$-Br)$_4${Cu(L^{o}-κ*P*)}$_4$] (5b and 6b)

$$CuBr + \mathbf{L^{p}} \longrightarrow [CuBr(\mathbf{L^{p}})]_n + [CuBr(\mathbf{L^{p}})]_4$$

Solution of **L^{p}** (57.5 mg, 0.2 mmol) in dichloromethane (5 mL) was added to a suspension of copper(I) bromide-dimethyl sulfide complex (41.1 mg, 0.2 mmol) in the same solvent (3 mL). The yellow mixture was stirred for 1 h and evaporated under vacuum. The solid residue was dissolved in a small amount of dichloromethane, the solution was filtered (PTFE syringe filter, 45 μm pore size) and layered with hexane. Crystallization by liquid-phase diffusion over several days afforded yellow crystals of **5b**·0.5CH_2Cl_2 and white crystals of **6b**·CH_2Cl_2 (3 mg, yield 3%). The crystals were isolated by suction and dried under vacuum. Yield of **5b**·1/3CH_2Cl_2: 40 mg (44%). Yield of **6b**·CH_2Cl_2: 3 mg (3%).

Characterization for **5b**·1/3CH_2Cl_2: ^{1}H NMR ($CDCl_3$): δ 7.27-7.34 (m, 4 H), 7.41-7.57 (m, 10 H). $^{31}P\{^1H\}$ NMR ($CDCl_3$): δ –8.5 (br s). IR (Nujol, cm^{-1}): 2241 w, 2230 m, 1589 m, 1308 w, 1180 w, 1158 w, 1098 s, 1071 w, 1027 w, 1017 w, 999 w, 972 w, 824 s, 748 s, 695 s, 643 w, 619 w, 582 w, 553 s, 512 s, 495 w, 485 w, 436 w, 410 w. ESI+ MS: *m/z* 637.0 ($[Cu(\mathbf{L^p})_2]^+$), 725.0 ($[Cu(\mathbf{L^p})_2BrK]^+$), 780.7 ($[Cu_2(\mathbf{L^p})_2Br]^+$). Anal. Calcd for $C_{19}H_{14}NBrCuP\cdot1/3CH_2Cl_2$ (459.0): C 50.58, H 3.22, N 3.05%. Found: C 50.33, H 3.19, N 2.75%.

Synthesis of [(μ$_3$-I)$_4${Cu(L^o-κ*P*)}$_4$] (6c)

$$CuI + \mathbf{L^p} \longrightarrow [CuI(\mathbf{L^p})]_4$$

Solution of $\mathbf{L^p}$ (19.0 mg, 0.10 mmol) in dichloromethane (6 mL) was added to a dichloromethane suspension of copper(I) iodide (28.7 mg, 0.10 mmol, in 2 ml). The yellow reaction mixture was stirred for 2 h and evaporated. The solid residue was dissolved in a small amount of ethyl acetate, the solution was filtered (PTFE syringe filter, 45 μm pore size) and layered with hexane. Crystallization by liquid-phase diffusion afforded yellow crystals of **6c**. Yield: 24 mg (50%).

Characterization: ^{1}H NMR ($CDCl_3$): δ 7.31-7.37 (m, 4 H), 7.46-7.58 (m, 10 H). $^{31}P\{^1H\}$ NMR ($CDCl_3$): δ −20.7 (br s). IR (Nujol, cm^{-1}): 3075 w, 3059 w, 2678 w, 2223 s, 1972 w, 1923 w, 1812 w, 1739 m, 1663 w, 1593 s, 1574 m, 1547 w, 1397 m, 1306 m, 1244 m, 1203 w, 1178 m, 1157 m, 1097 s, 1069 w, 1047 w, 1031 m, 1015 m, 998 w, 97 w, 958 w, 918 w, 845 w, 827 s, 753s, 706w, 692 s, 620 w, 585 s, 554 s, 503 s, 488 m, 420 w. ESI+ MS: *m/z* 637.1 ($[Cu(\mathbf{L^p})_2]^+$). Anal. Calcd for $C_{76}H_{56}N_4Cu_4I_4P_4$ (477.73): C 47.77, H 2.95, N 2.93% Found: C 48.03, H 3.05, N 2.48%.

Synthesis of [{μ(C,N)-CN}Cu(L^o-κ*P*)]$_n$ (7)

$$CuCN + \mathbf{L^o} \longrightarrow [CuCN(\mathbf{L^o})]_n$$

Solution of $\mathbf{L^o}$ (71.8 mg, 0.25 mmol) in dichloromethane (7 mL) was added to a dichloromethane suspension of copper(I) cyanide (22.4 mg, 0.25 mmol, in 2 ml) and resulting colorless mixture was stirred for 2.5 h and then evaporated. The crude product was taken up with a small amount of dichloromethane. The solution was filtered (PTFE syringe

filter, 45 µm pore size) and layered with hexane. Crystallization by liquid-phase diffusion over 7 days provided colorless crystals of **7.** The crystals were isolated by suction and dried under vacuum. Yield of **7**·1/10CH_2Cl_2: 66 mg (68%).

Characterization: NMR ($CDCl_3$): ^{1}H NMR ($CDCl_3$): δ 7.09-7.14 (m, 1 H), 7.32-7.51 (m, 12 H), 7.64-7.68 (m, 1 H). $^{31}P\{^1H\}$ δ −7.0 (s). IR (Nujol, cm^{-1}): 3049 w, 2674 w, 2227 m, 2128 s, 1585 w, 1307 w, 1283 w, 1193 w, 1165 w, 1129 w, 1096 m, 1068 w, 1027 w, 999 w, 919 w, 847 w, 765 s, 752 s, 745 s, 727 w, 707 w, 695 s, 674 w, 581 m, 527 s, 505 s, 494 s, 478 w, 436 w, 407 w. ESI+ MS: *m/z* 726.0 ($[Cu_2CN(\mathbf{L^o})_2]^+$). Anal. Calcd for $C_{20}H_{14}N_2CuP$·1/10CH_2Cl_2 (385.3): C 62.65, H 3.71, N 7.27 % Found: C 62.72, H 3.64, N 6.95 %.

Synthesis of [{µ(P,N)-L^o}$_2${Cu(H_2O)(MeCN)}$_2$][BF_4]$_2$ (8)

$$[Cu(MeCN)_4][BF_4] + \mathbf{L^o} \longrightarrow [Cu(MeCN)(H_2O)(\mathbf{L^o})]_2[BF_4]_2$$

Solution of $\mathbf{L^o}$ (57.4 mg, 0.20 mmol) in dichloromethane (10 mL) was added to suspension of tetrakis(acetonitrile)copper(I) tetrafluoroborate (57.4 mg, 0.20 mmol) in the same solvent (5 mL). After stirring for 6 h, the reaction mixture was evaporated, yields a residue which was dissolved in small amount of ethyl acetate. The solution was filtered (PTFE syringe filter, 45 µm pore size) and layered with hexane. Crystallization by liquid-phase diffusion gave colorless crystals of **8**. Yield: 59.0 mg (62 %).

Characterization: ^{1}H NMR (CD_3COCD_3): δ 2.21 (s, 3 H, MeCN), 3.10 (br s, 2 H, H_2O), 7.08-7.16 (m, 1 H), 7.44-7.68 (m, 10 H), 7.80-7.90 (m, 2 H), 8.18-8.26 (m, 1 H). $^{31}P\{^1H\}$ NMR (CD_3COCD_3): δ −0.91 (br s). IR (Nujol, cm^{-1}): 3049 w, 2308 w, 2278 w, 1840 w, 1630 br m, 1586 w, 1308 w, 1284 w, 1194 m, 11302 m, 1097 s, 1068 s, 1068 s, 1034 s, 1023 s, 998 s, 961 m, 885 w, 788 w, 770 s, 754 s, 445 s. 708 m, 694 s, 673 w, 580 m, 540s, 513 m, 499 s, 436 w. ESI+ MS: *m/z* 637.0 ($[Cu(\mathbf{L^o})_2]^+$). Anal. Calcd for $C_{42}H_{38}N_4B_2Cu_2F_8O_2P_2$ (993.4): C 50.78, H 3.86, N 5.64% Found: C 50.80, H 3.68, N 5.49%.

Synthesis of [{μ(P,N)-L^o}$_2$Cu]$_3$[BF$_4$]$_3$ (9)

$$[Cu(MeCN)_4][BF_4] + 2\ \mathbf{L^o} \longrightarrow [Cu_3(\mathbf{L^o})_6][BF_4]_3$$

Solution of **L^o** (57.4 mg, 0.20 mmol) in dichloromethane (4 mL) was added to a suspension of tetrakis(acetonitrile)copper(I) tetrafluoroborate (31.5 mg, 0.1 mmol) in the same solvent (3 mL). The resulting mixture was stirred for 2 h. The solid residue obtained after evaporation was dissolved in a small amount of dichloromethane, the solution was filtered (PTFE syringe filter, 45 μm pore size) and layered with hexane. Crystallization by liquid-phase diffusion gave white crystals of **9**·CH_2Cl_2. Yield: 54 mg (72%).

Characterization: ^{1}H NMR (CD_2Cl_2): δ 6.02-6.042 (m, 1 H), 6.52-6.60 (m, 2H), 6.95-7.78 (m, 23 H), 7.80-781 (m, 1 H), 8.02-8.07 (m, 1 H). ^{31}P{^{1}H} NMR (CD_2Cl_2): δ −2.0 (s) and −3.3 (br s). ESI+ MS: *m/z* 637.0 ([Cu(**L^o**)$_2$]$^+$). IR (Nujol, cm^{-1}): 2236 w, 1653 w, 1580 w, 1481 w, 1436 s, 1312 w, 1286 w, 1197 w, 1160 w, 1092 s, s 1059 s, 1000 m, 765 m, 752 m, 744 m, 723 w, 698s. Anal. Calcd for $C_{114}H_{84}N_6B_3Cu_3F_{12}P_6 \cdot CH_2Cl_2$ (2259.7): C 61.12, H 3.84, N 3.72% Found: C 61.48, H 3.92, N 3.65%.

Synthesis of [{μ(P,N)-L^o}$_2${Cu(MeO-L^o-κ*P*)}$_2$][BF$_4$]$_2$ (10)

$$[Cu(MeCN)_4][BF_4] + 2\ \mathbf{L^o} \longrightarrow [Cu(\mathbf{L^o})(MeO\text{-}\mathbf{L^o})]_2[BF_4]_2$$

Solution of **L^o** (86.2 mg, 0.30 mmol) in dichloromethane (2 mL) was added to a suspension of tetrakis(acetonitrile)copper(I) tetrafluoroborate (47.2 mg, 0.15 mmol) in the methanol (4 mL). The resulting mixture was refluxed in argon atmosphere for 6 h. The solid residue obtained after evaporation was dissolved in a small amount of chloroform, the solution was filtered (PTFE syringe filter, 45 μm pore size) and layered with hexane. Crystallization by liquid-phase diffusion gave white crystals of **10**·6$CHCl_3$. The crystals were isolated by suction and dried under vacuum. Yield of **10**: 15 mg (13%).

Characterization: ESI+ MS: *m/z* 382.0 ([Cu(MeO-**L**^{o})]$^{+}$), 637.0 ([Cu(**L**^{o})$_2$]$^{+}$), 669.0 ([Cu(**L**^{o})(MeO-**L**^{o})]$^{+}$). 701.0 ([Cu(MeO-**L**^{o})$_2$]$^{+}$). IR (Nujol, cm^{-1}): 3288 m, 2238 w, 1643 m, 1585 w, 1559 w, 1541 w, 1309 w, 1287 w, 1202 w, 1187 w, 1164 w, 1134 w, 1114 w, 1066 s, 1030 m, 997 w, 805 w, 777 w, 748 w, 724 w, 698 m, 669 w, 579 w, 501 m, 482 w, 430 w, 412 w. Anal. Calcd for $C_{78}H_{64}N_4B_4Cu_4F_8O_2P_4$ (1513.9): C 61.88, H 4.26, N 3.70% Found: C 61.68, H 4.62, N 3.43%.

5. Attachments

5.1 Crystallographic data

Crystallographic data, data collection and structure refinement parameters for prepared complexes are listed in Table 5.1, 5.2, 5.3 and 5.4.

Table 5.1: Crystallographic data, data collection and structure refinement parameters for **L^p**, **1**, **2** and **3**.

Compound	**L^p**	**1**	**2**	**3**·2CHCl$_3$
Formula	$C_{19}H_{14}NP$	$C_{57}H_{42}Cl_4Cu_4N_3P_3$	$C_{76}H_{56}Br_4Cu_4N_4P_4$	$C_{38}H_{28}Cu_3I_3N_2P_2$·2 $CHCl_3$
M [g/mol]	287.28	1257.81	1722.93	1503.99
Crystal system	monoclinic	triclinic	triclinic	monoclinic
Space group	*P*2$_1$/*n* (no. 14)	*P*-1 (no. 2)	*P*-1 (no. 2)	*C*2/*c* (no. 15)
a [Å]	9.6939(2)	11.3832(2)	10.5092(3)	19.2696(5)
b [Å]	15.7842(4)	15.4185(3)	11.7864(3)	16.1991(3)
c [Å]	10.7560(2)	19.9852(4)	14.8827(4)	17.8699(4)
α [°]		86.781(1)	87.923(1)	
β [°]	115.743(1)	88.440(1)	74.051 (1)	114.522(1)
γ [°]		89.396(1)	78.127(1)	114.522(1)
V [Å^3]	1482.44(6)	3500.66(12)	1734.17(8)	5075.0(2)
Z	4	2	1	4
D_{calc} [g/cm^3]	1.287	1.193	1.650	1.968
F(000)	312	1268	856	2880
Collected diffractions	13940	53526	22770	18641
R_{int} [%][a]	2.60	2.48	2.29	3.80
Independent diffractions	2890	16054	7976	5829
Observed diffractions	2657	12732	6724	4508
R (observed diffractions) [%][c]	3.11	3.08	2.39	3.38
R (all diffractions) [%][c]	3.39	4.05	3.30	5.03
wR (all diffractions) [%][d]	8.12	7.94	5.61	8.18
Δρ [e Å^{-3}]	0.23; –0.29	0.48; –0.40	0.41; –0.43	1.13; –1.00

Table 5.2: Crystallographic data, data collection and structure refinement parameters for **4a-c** and **5a**.

Compound	**4a**	**4b**	**4c**	**5a**·2$CHCl_3$
Formula	$C_{38}H_{28}ClCuN_2P_2$	$C_{38}H_{28}BrCuN_2P_2$	$C_{38}H_{28}CuIN_2P_2$	$C_{19}H_{14}ClCuNP\cdot 2CHCl_3$
M [g/mol]	673.55	718.01	765.00	625.01
Crystal system	monoclinic	triclinic	monoclinic	monoclinic
Space group	*C*2/*c* (no. 15)	*P*-1 (no. 2)	*C*2/*c* (no. 15)	*P*21/*n* (no. 14)
a [Å]	20.4046(5)	9.9490(2)	19.0763(3)	13.1063(3)
b [Å]	10.0455(2)	10.4805(2)	9.8794(2)	10.2714(3)
c [Å]	17.0571(4)	17.6769(4)	19.684(3)	20.1935(5)
α [°]		81.782(1)		
β [°]	109.185(9)	78.027(1)	117.686(7)	98.921(1)
γ [°]		65.535(1)		
V [Å^3]	3302.09(13)	1637.82(6)	3284.87(10)	2685.50(12)
Z	4	2	4	4
D_{calc} [g/cm^3]	1.355	1.456	1.547	1.546
F(000)	1384	728	1528	1248
Collected diffractions	20888	24906	10518	17292
R_{int} [%][a]	4.28	2.05	1.71	2.40
Independent diffractions	3797	7516	3595	5279
Observed diffractions	3073	6480	3234	4088
R (observed diffractions) [%][c]	3.16	2.82	2.24	5.06
R (all diffractions) [%][c]	4.52	3.56	2.62	6.71
wR (all diffractions) [%][d]	6.77	6.47	5.65	13.8
$\Delta\rho$ [e Å^{-3}]	0.39; –0.24	1.43; –1.05	0.41, –0.47	1.01; –0.94

Table 5.3: Crystallographic data, data collection and structure refinement parameters for **5b**, **6b-c** and **7**.

Compound	2 **(5b)**·CH_2Cl_2	**6b**·CH_2Cl_2	**6c**	**7**
Formula	2 ($C_{19}H_{14}BrCuNP$) · CH_2Cl_2	$C_{76}H_{56}Br_4Cu_4N_4$ · CH_2Cl_2	$C_{76}H_{56}Cu_4I_4$ N_4P_4	$C_{20}H_{14}CuN_2P$
M [g/mol]	946.39	1807.85	1910.89	376.84
Crystal system	triclinic	orthorhombic	tetragonal	monoclinic
Space group	P-1 (no. 2)	$C222_1$ (no. 20)	$I4_1/a$ (no. 88)	$P2_1/c$ (no. 14)
a [Å]	10.2501(2)	15.0323(7)	21.8593(6)	10.6218(2)
b [Å]	11.5577(2)	19.5583(9)	21.8593(6)	18.8904(3)
c [Å]	17.3967(3)	25.1167(12)	14.9540(4)	8.9534(2)
α [°]	105.894(1)			
β [°]	96.247(1)			105.896(1)
γ [°]	98.958(1)			
V [Å^3]	1932.94(6)	7384.5(6)	7145.5(3)	1727.81(6)
Z	2	4	4	4
D_{calc} [g/cm^3]	1.626	1.626	1.776	1.449
F(000)	940	3592	3712	768
Collected diffractions	29574	26444	20110	13483
R_{int} [%][a]	3.05	5.23	3.58	1.80
Independent diffractions	8874	7174	4101	3961
Observed diffractions	6701	6486	3379	3538
R (observed diffractions) [%][c]	3.74	4.29	2.69	2.49
R (all diffractions) [%][c]	5.65	4.92	3.77	2.95
wR (all diffractions) [%][d]	10.5	9.19	6.35	6.49
Δρ [e Å^{-3}]	1.57; –0.69	0.94; –0.66	0.70; –0.34	0.35; –0.30

Table 5.4: Crystallographic data, data collection and structure refinement parameters for **8**, **9** and **10**.

Compound	**8**	**9**·CH_2Cl_2	**10**·6$CHCl_3$
Formula	$C_{42}H_{38}B_2Cu_2F_8N_4O_2P_2$	$C_{114}H_{83}B_3Cu_3F_{12}N_6P_6 \cdot CH_2Cl_2$	$C_{78}H_{64}B_2Cu_2F_8N_4\ O_2P_4 \cdot 6\ CHCl_3$
M [g/mol]	993.40	2258.65	2230.12
Crystal system	monoclinic	monoclinic	triclinic
Space group	$P2_1/c$ (no. 14)	Cc (no. 9)	P-1 (no. 2)
a [Å]	12.5469(2)	25.1774(7)	13.8949(5)
b [Å]	9.2121(2)	23.5784(6)	14.8300(6)
c [Å]	19.7221(4)	19.5647(5)	14.9456(6)
α [°]			118.749(1)
β [°]	101.253(1)	101.043(1)	98.180(1)
γ [°]			108.171(2)
V [Å^3]	2235.72(8)	11399.4(5)	2402.3(2)
Z	2	4	1
D_{calc} [g/cm^3]	1.476	1.316	1.541
F(000)	1008	4604	1124
Collected diffractions	19081	77193	67891
R_{int} [%][a]	1.72	3.56	2.26
Independent diffractions	5123	22403	11054
Observed diffractions	4578	20852	9313
R (observed diffractions) [%][c]	2.70	3.95	3.62
R (all diffractions) [%][c]	3.15	4.37	5.66
wR (all diffractions) [%][d]	7.32	10.7	8.95
$\Delta\rho$ [e Å^{-3}]	0.64; –0.31	1.45; –1.01	0.78; –0.67

[a] $R_{\text{int}} = \sum \left| F_o^2 - \langle F_o^2 \rangle \right| / \sum F_o^2$

[b] $I_o \geq 2\sigma(I_o)$

[c] $R = (|F_o| - |F_c|) / \sum |F_o|$

[d] $wR = \{ \sum \left[w(F_o{}^2 - F_c{}^2)^2 \right] / \sum w(F_o{}^2)^2 \}^{1/2}$, where $w = [\sigma^2 F_o^2 + (w_1 P)^2 + w_2 P]^{-1}$, $P = (F_o{}^2 + 2F_c{}^2)/3$

6. References

(1) Seebach, D. *Angew. Chem.* **1990**, *102*, 1363.

(2) Seebach, D. *Angew. Chem. Int. Ed.* **1990**, *29*, 1320.

(3) Beller, M. *Angew. Chem. Int. Ed.* **1995**, *34*, 1316.

(4) Evano, G.; Blanchard, N.; Toumi, M. *Chem. Rev.* **2008**, *108*, 3054.

(5) Kolb, H. C.; Finn, M. G.; Sharpless, K. B. *Angew. Chem. Int. Ed.* **2001**, *40*, 2004.

(6) Majumder, N. *I JRPC* **2015**, *5*, 95.

(7) Huisgen, R. *Angew. Chem.* **1963**, *75*, 604.

(8) Huisgen, R. *Angew. Chem. Int. Ed.* **1963**, *2*, 565.

(9) Haldon, E.; Nicasio, M. C.; Perez, P. J. *Org. Biomol. Chem.* **2015**, *13*, 9528.

(10) Harris, F.; Pierpoint, L. *Med. Res. Rev.* **2012**, *29*, 1292.

(11) Bourne, Y.; Kolb, H. C.; Radić, Z.; Sharpless, K. B.; Taylor, P.; Marchot, P. *PNAS* **2004**, *101*, 1449.

(12) Whiting, M.; Muldoon, J.; Lin, Y.-C.; Silverman, S. M.; Lindstrom, W.; Olson, A. J.; Kolb, H. C.; Finn, M. G.; Sharpless, K. B.; Elder, J. H.; Fokin, V. V. *Angew. Chemie Int. Ed.* **2006**, *45*, 1435.

(13) Tornøe, C. W.; Sanderson, S. J.; Mottram, J. C.; Coombs, G. H.; Meldal, M. *J. Comb. Chem.* **2004**, *6*, 312.

(14) Voit, B. *New J. Chem.* **2007**, *31*, 1139.

(15) Fournier, D.; Hoogenboom, R.; Schubert, U. S. *Chem. Soc. Rev.* **2007**, *36*, 1369.

(16) Hänni, K. D.; Leigh, D. A. *Chem. Soc. Rev.* **2010**, *39*, 1240.

(17) Haldon, E.; Nicasio, M. C.; Perez, P. J. *Org. Biomol. Chem.* **2015**, *13*, 9528.

(18) Chan, T. R.; Hilgraf, R.; Sharpless, K. B.; Fokin, V. V. *Org. Lett.* **2004**, *6*, 2853.

(19) Lewis, W. G.; Magallon, F. G.; Fokin, V. V.; Finn, M. G. *J. Am. Chem. Soc.* **2004**, *126*, 9152.

(20) Jiang, H.; Zheng, T.; Lopez-Aguilar, A.; Feng, L.; Kopp, F.; Marlow, F. L.; Wu, P. *Bioconjug. Chem.* **2014**, *25*, 698.

(21) Pérez-Balderas, F.; Ortega-Muñoz, M.; Morales-Sanfrutos, J.; Hernández-Mateo, F.; Calvo-Flores, F. G.; Calvo-Asín, J. A.; Isac-García, J.; Santoyo-González, F. *Org. Lett.* **2003**, *5*, 1951.

(22) Lal, S.; McNally, J.; White, A. J. P.; Díez-González, S. *Organometallics* **2011**, *30*, 6225.
(23) Díez-González, S.; Correa, A.; Cavallo, L.; Nolan, S. P. *Chem. Eur. J.* **2006**, *12*, 7558.
(24) Fanta, P. A. *Synthesis* **1974**, *1*, 9.
(25) Jones, G. O.; Liu, P.; Houk, K. N.; Buchwald, S. L. *J. Am. Chem. Soc.* **2010**, 1.
(26) Das, B.; Salvanna, N.; Reddy, G. C.; Balasubramanyam, P. *Tetrahedron Lett.* **2011**, *52*, 6497.
(27) Zeng, C.; Wang, N.; Peng, T.; Wang, S. *Inorg. Chem.* **2017**, *56*, 1616.
(28) Ford, P. C.; Cariati, E.; Bourassa, J. *J. Chem. Rev.* **1999**, *99*, 3625.
(29) Xu, H.; Chen, R.; Sun, Q.; Lai, W.; Su, Q.; Huang, W.; Liu, X. *Chem. Soc. Rev.* **2014**, *43*, 3259.
(30) Ford, P. C.; Cariati, E.; Bourassa, J. *Chem. Rev.* **1999**, *99*, 3625.
(31) Kobayashi, A.; Arata, R.; Ogawa, T.; Yoshida, M.; Kato, M. *Inorg. Chem.* **2017**, *56*, 4280.
(32) Rosenberg, B.; Camp, L.; Krigas, T. *Nature* **1965**, 698.
(33) Lopes, J.; Alves, D.; Morais, T. S.; Costa, P. J.; Piedade, M. F. M.; Marques, F.; Villa de Brito, M. J.; Helena Garcia, M. *J. Inorg. Biochem.* **2017**, *169*, 68.
(34) Puig, S.; Thiele, D. J. *Curr. Opin. Chem. Biol.* **2002**, *6*, 171.
(35) Marzano, C.; Pellei, M.; Tisato, F.; Santini, C. *Anticancer. Agents Med. Chem.* **2009**, *9*, 185.
(36) Santini, C.; Pellei, M.; Gandin, V.; Porchia, M.; Tisato, F.; Marzano, C. *Chem. Rev.* **2014**, *114*, 815.
(37) Raston, C. L.; White, A. H. *Dalton Trans.* **1976**, 2153.
(38) Rath, N. P.; Maxwell, J. L.; Holt, E. M. *Dalton Trans.* **1986**, 2449.
(39) Dyason, J. C.; Healy, P. C.; Pakawatchai, I. C.; Patrick, V. A.; Ib, A. H. W. *Inorg. Chem.* **1985**, 1957.
(40) Eitel, E.; Oelkrug, D.; Hiller, W.; Strahle, J. *Naturforsch* **1980**, 35b, 1247.
(41) Schrock, R. R.; Osborn, J. A. *J. Am. Chem. Soc.* **1976**, *98*, 2134.
(42) Bader, A.; Lindner, E. *Coord. Chem. Rev.* **1991**, *108*, 27.
(43) Crabtree R. H. *The Organometallic Chemistry of the Transition Metals*, Fourth Ed.; Wiley; **2005**.
(44) Pearson, R. G. *J. Am. Chem. Soc.* **1963**, *85*, 3533.
(45) Tolman, C. *Chem. Rev.* **1977**, *77*, 313.
(46) Borns, S.; Kadyrov, R.; Heller, D.; Baumann, W.; Spannenberg, A.; Kempe, R.; Holz,

J.; Börner, A. *Eur. J. Inorg. Chem.* **1998**, 1291.

(47) Štěpnička, P. *Chem. Soc. Rev.* **2012**, *41*, 4273.

(48) Michelin, R. A.; Mozzon, M.; Bertani, R. *Coord. Chem. Rev.* **1996**, *147*, 299.

(49) Klasen, C.; Lorenz, I.; Schmid, S. *J. Organomet. Chem.* **1992**, *428*, 363.

(50) Sithole, S. V.; Staples, R. J.; Van Zyl, W. E. *Inorg. Chem. Commun.* **2012**, *15*, 216.

(51) Maraval, A.; Owsianik, K.; Arquier, D.; Igau, A.; Coppel, Y.; Donnadieu, B.; Zablocka, M.; Majoral, J. *Eur. J. Inorg. Chem.* **2003**, 960.

(52) Škoch, K.; Císařová, I.; Štěpnička, P. *Inorg. Chem.* **2014**, *53*, 568.

(53) Payne, D. H.; Payne, Z. A.; Rohmer, R.; Frye, H. *Inorg. Chem.* **1973**, *12*, 2540.

(54) Payne, D. H.; Frye, H. *Inorg. Nucl. Chem. Lett.* **1972**, *8*, 73.

(55) Škoch, K.; Uhlík, F.; Císařová, I.; Štěpnička, P. *Dalton Trans.* **2016**, *45*, 10655.

(56) Škoch, K.; Císařová, I.; Štěpnička, P. *Chem. Eur. J.* **2015**, *21*, 15998.

(57) Reis, A.; Dehe, D.; Farsadpour, S.; Munstein, I.; Sun, Y.; Thiel, W. R. *New J. Chem.* **2011**, *35*, 2488.

(58) Baltzer, N.; Macko, L.; Schaffner, S.; Zehnder, M. *Helv. Chim. Acta* **1996**, *79*, 803.

(59) Taborsky, P.; Necas, M.; Bartos, P. *Sulfur Slicon Relat. Elem.* **2016**, *191*, 645.

(60) Nishimura, M.; Ueda, M.; Norio, M. *Tetrahedron* **2002**, *58*, 5779.

(61) Reis, A.; Dehe, D.; Farsadpour, S.; Munstein, I.; Sun, Y.; Thiel, W. R. *New J. Chem.* **2011**, *35*, 2488.

(62) Bowmaker, G. A.; Hart, S. R. D.; Jones, B. E.; Skeltonb, B. W.; Whiteb, A. H. *J. Chem. Soc. Dalton Trans.* **1995**, 3063.

(63) Churchill, M. R.; Kalra, K. L. *Inorg. Chem.* **1974**, *13*, 1427.

(64) Chen, B.; Mok, K.; Ng, S. *J. Chem. Soc. Dalton Trans.* **1998**, *1*, 2861.

(65) Steyl, G. *Acta Crystallogr.,Sect. E: Struct. Rep. Online* **2006**, *62*, m3277.

(66) Mamais, M.; Cox, P. J.; Aslanidis, P. *Polyhedron* **2008**, *27*, 175.

(67) Qi, L.; Li, Q.; Hong, X.; Liu, L.; Zhong, X.-X.; Chen, Q.; Li, F.-B.; Liu, Q.; Qin, H.-M.; Wong, W.-Y. *J. Coord. Chem.* **2016**, *69*, 3692.

(68) Vega, A.; Saillard, J. Y. *Inorg. Chem.* **2004**, *43*, 4012.

(69) Lin, Y. Y.; Lai, S. W.; Che, C. M.; Fu, W. F.; Zhou, Z. Y.; Zhu, N. *Inorg. Chem.* **2005**, *44*, 1511.

(70) Choubey, B.; Radhakrishna, L.; Mague, J. T.; Balakrishna, M. S. *Inorg. Chem.* **2016**, *55*, 8514.

(71) Bowmaker, G. a.; Kennedy, B. J.; Reid, J. C. *Inorg. Chem.* **1998**, *37*, 3968.

(72) Hathaway, B. J.; Holah, D. G.; Underhill, A. E. *J. Chem. Soc.* **1962**, 2444.

(73) Worrell, B. T.; Malik, J. A.; Fokin, V. V. *Science* **2013**, *340*, 457.

(74) Nobbs, J. H. *Rev. Prog. Color.* **1985**, *15*, 66.

(75) Hashimoto, M.; Igawa, S.; Yashima, M.; Kawata, I.; Hoshino, M.; Osawa, M. *J. Am. Chem. Soc.* **2011**, *133*, 10348.

(76) Tsuboyama, A.; Kuge, K.; Furugori, M.; Okada, S.; Hoshino, M.; Ueno, K. *Inorg. Chem.* **2007**, *46*, 1992.

(77) Evans, D. R.; Reed, C. A. *J. Am. Chem. Soc.* **2000**, *122*, 4660.

(78) Shriver, D. F.; Drezdzon, M. A. *The Manipulation of Air-Sensitive Compounds*; Second Ed.; Wiley; **1986**.

(79) Sheldrick, G. M. *Acta Crystallogr. Sect. A: Found. Crystallogr.* **2008**, *64*, 112.

(80) Spek, A. L. *Acta Crystallogr. Sect. C: Struct. Chem.* **2015**, *71*, 9.